FONDAZIONE
BRUNO KESSLER

Non-standard noise sources in silicon microstrip detectors

Gabriele Giacomini
BNL, April 30th 2014

Outline

- silicon sensor activity in FBK
- excess noise in silicon microstrip detectors:
  - $ENC^2 \sim sqrt(\tau)$
  - $ENC^2 \sim I^2_{PT}\,\tau^2$
  - thermal noise

Outline

- silicon sensor activity in FBK

- excess noise in silicon microstrip detectors:
  - $ENC^2 \sim sqrt(\tau)$
  - $ENC^2 \sim I^2_{PT}\,\tau^2$
  - thermal noise

FONDAZIONE
BRUNO KESSLER

Fondazione Bruno Kessler

Centre for Materials and Microsystems

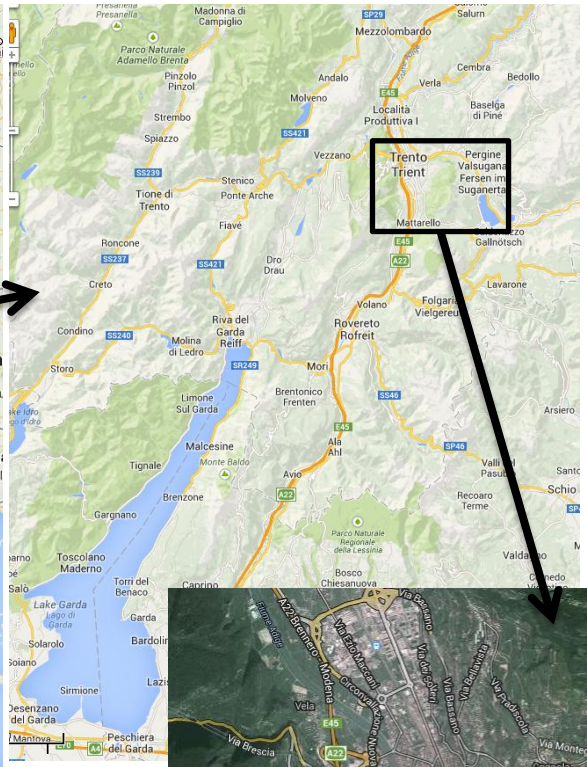

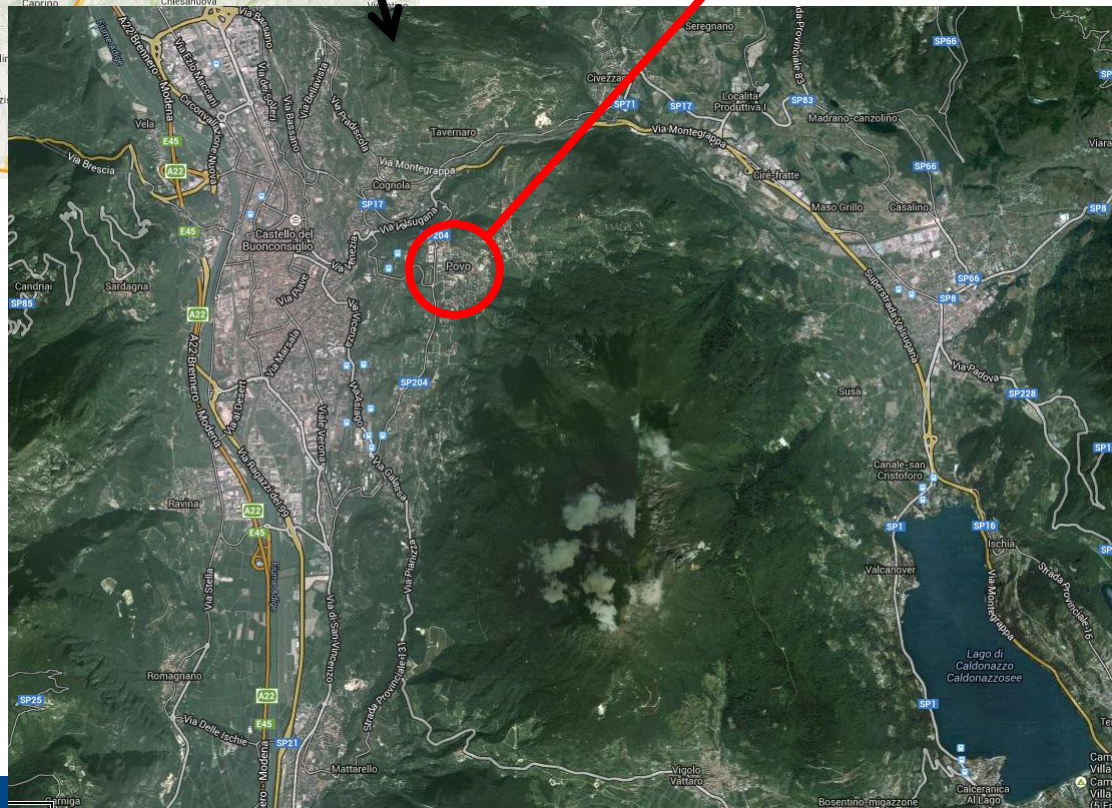
Povo
Castello del Buonconsiglio
Tavernaro
Cognola
Via Montegrappa
Via Brescia
Via Lasugana
Via Venezia
Via Rovere
Via Manzoni
Via Bassano
Via Bolzano
Via Pedemonte
Via Ravina
Via Stella
Via Delle Ischie
Via di San Vincenzo
Via Pianzera
Via Caldesa
Via Verona
Via Lagarina
Via Padova
Via Montegrappa
Via Prati
Via Pedemonte
Via Bassano
Via Bolzano
Via Rolandino
Via Ischia
Via Montegrappa

FONDAZIONE
BRUNO KESSLER

Centre for Materials and Microsystems

MTLab Fabrication Facility

Pierluigi Bellutti
bellutti@fbk.eu

Silicon Facility Expertise

TCAD simulation
CAD design

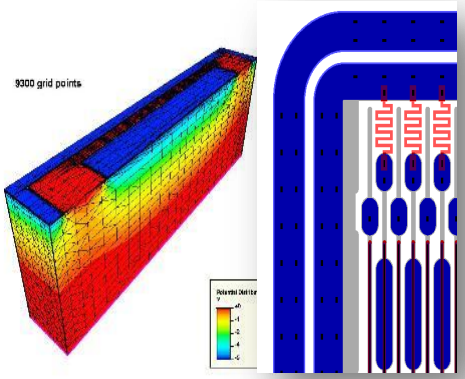

Fabrication

Device testing

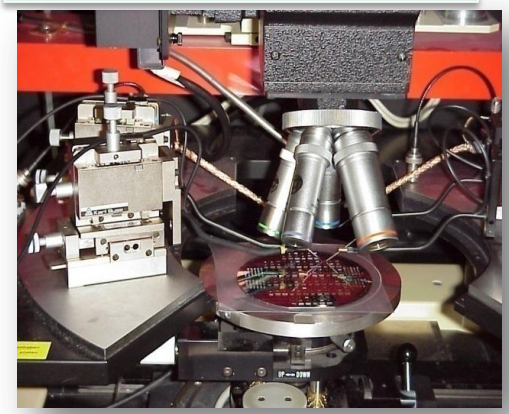

Material Characterization:

- XPS
- SIMS
- ToF-SIMS
- TXRF
- AFM
- SEM

Custom CMOS design

Development of ROIC by exploiting state of the art CMOS tech (external services)

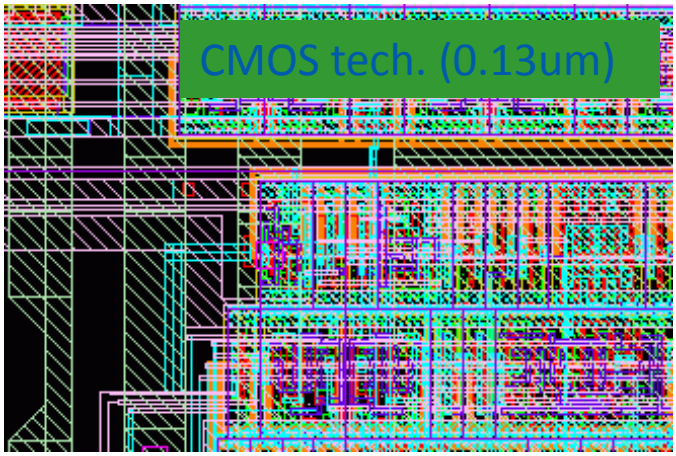

MTLab Facility: MicroFabrication Area

Two separate clean rooms

- 500m^2 of clean room (class 10-100)
- 200m^2 of clean area (class 100-1000) equipped for MEMS technology

6-inch wafers (Si, Quartz, Glass) – 0.35 um processing

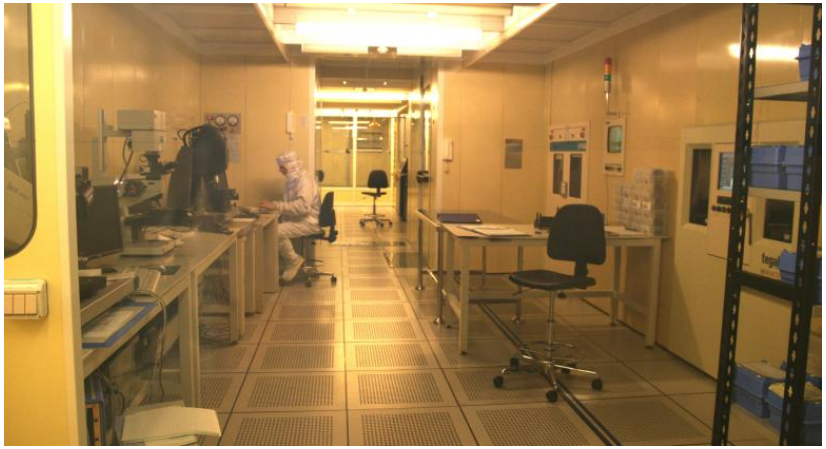

- Dry/wet oxidation
- sputtering Metallization
- Diffusion
- LPCVD
- PECVD
- Projection lithography: CD 2um, accuracy 1um
- Stepping lithography: CD 350nm, accuracy 75nm
- Ion Implantation
- Dry/wet etching

MTLab Facility: Testing Area

Four labs

- 20m^2 for manual parametric testing (2 probers)
- 15m^2 for solar cells qualification
- 60 m^2 for automatic parametric/functional testing (4 probers)
- 20 m^2 optical testing

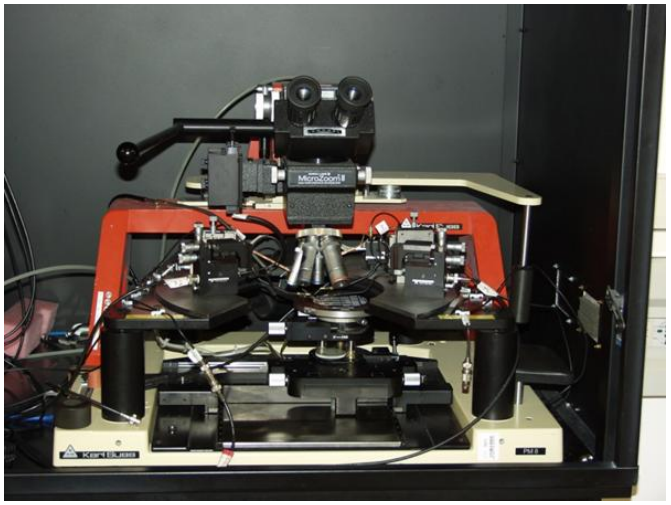

More than 11000 hours/year

FONDAZIONE BRUNO KESSLER

SRS SILICON RADIATION SENSORS

Centre for Materials and Microsystems

Silicon Radiation Sensors

IRIS

Integrated Radiation and Image Sensors

Claudio Piemonte

piemonte@fbk.eu

srs.fbk.eu

SRS activity

Development of silicon radiation sensors

Sensors on high-resistivity substrates

- pixel detectors
- strip detectors
- drift detectors
- 3D detectors

Sensors with internal gain for light detection

- Silicon Photomultipliers
- SPADs

Pixel detectors: examples

Medipix 1&2

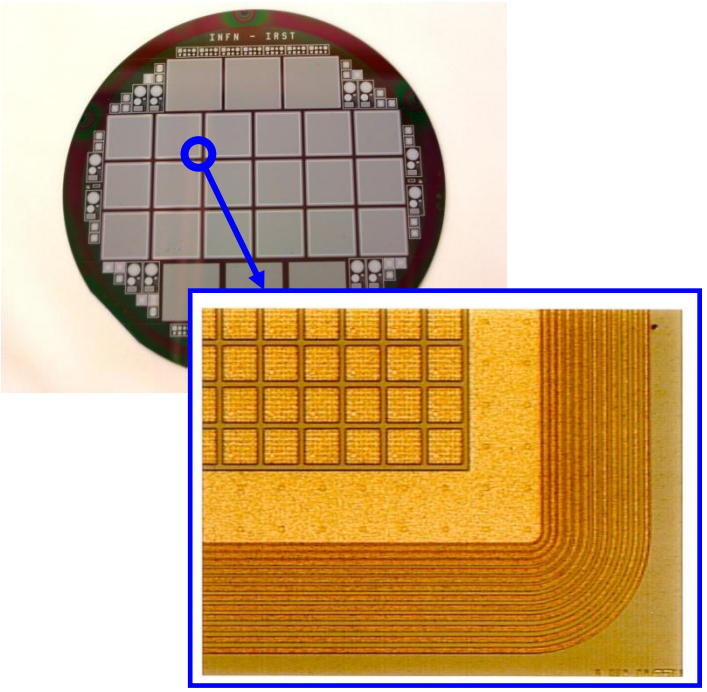

- Medipix1: pixel size 170x170um^2
- Medipix2: pixel size 55x55um^2

Substrate thick.: up to 1.5mm

NA48/ALICE experiment

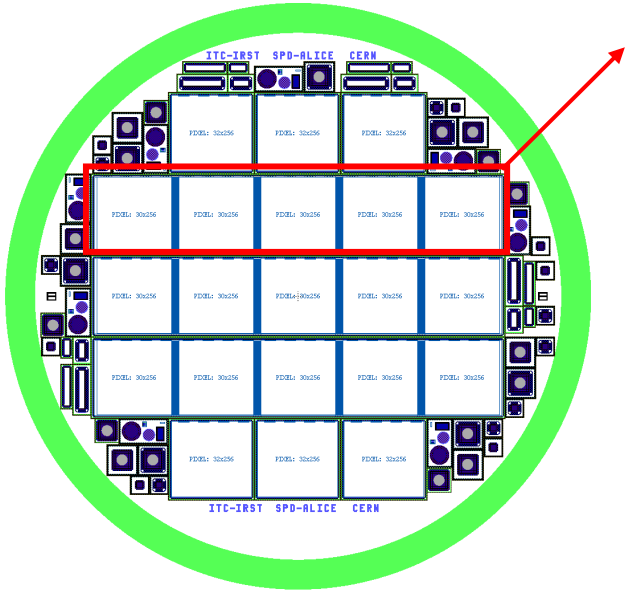

ladder

- ALICE SPD layout
- pixel size 50x400um^2

Substrate thickness: 200μm

Leakage current ~100pA/cm^2 for 300um substrates

Thick Pad detectors: example

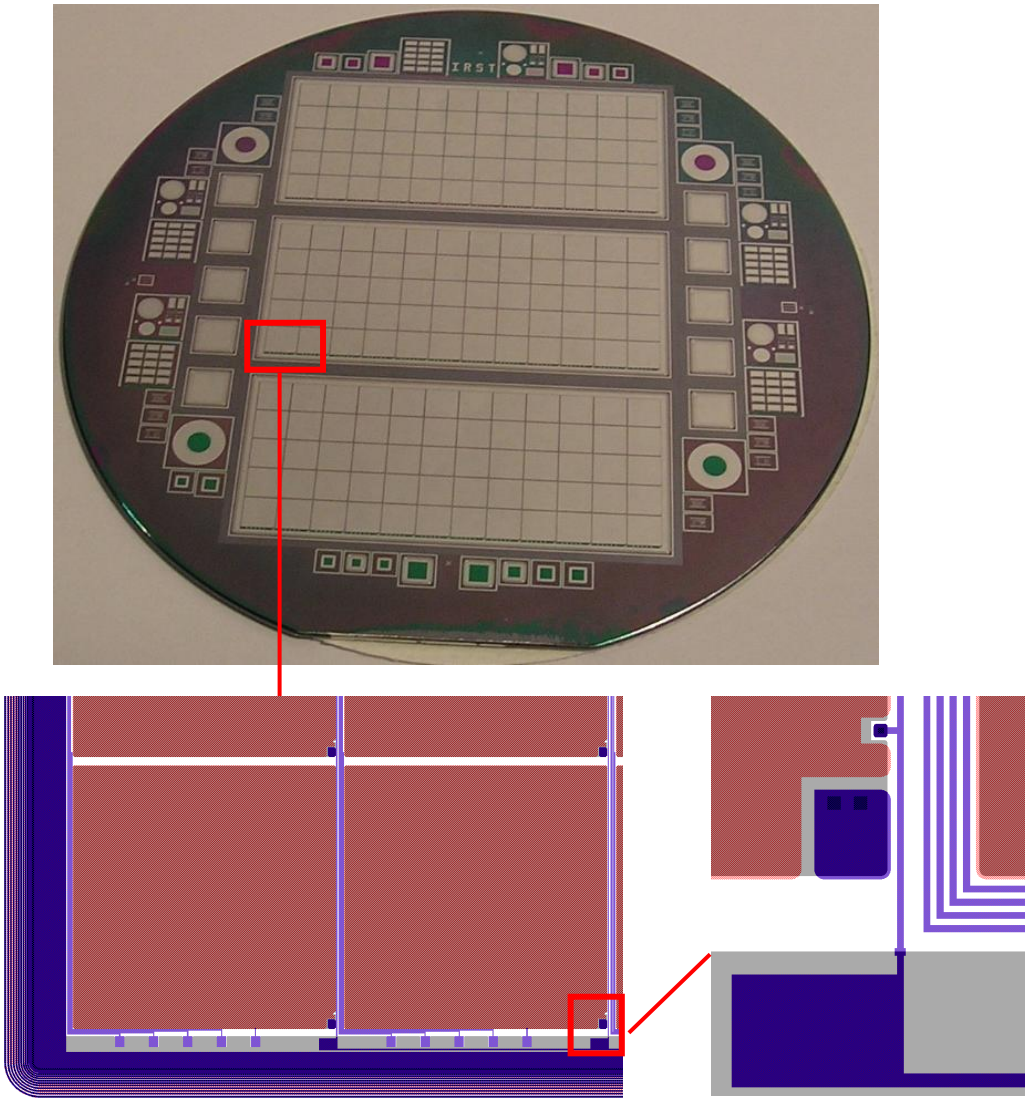

1.5mm-thick wafer
(also 200µm-thick, same design)

PAD detectors:

- 12x5 elements
- 4mm pitch (X and Y)
- AC coupling
- punch-through biasing
- termination structure
  (voltage handling, lateral depletion)

Strip Detectors: productions

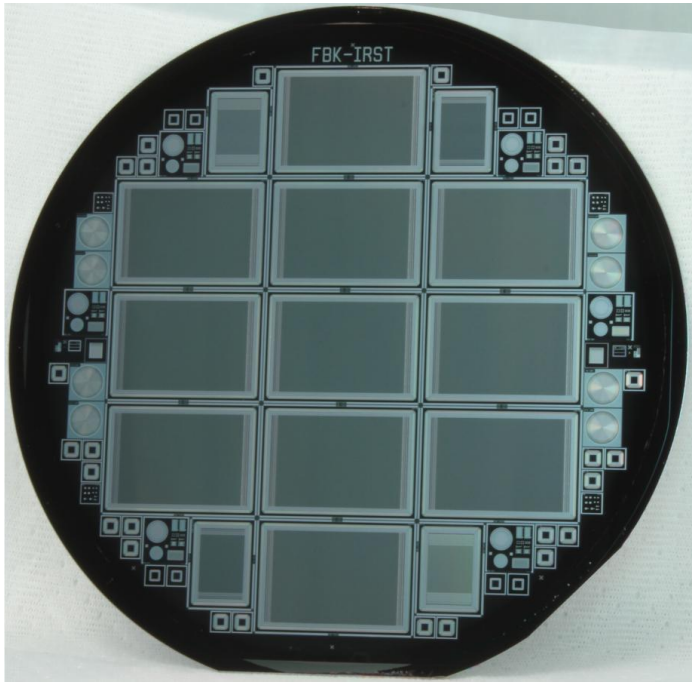

Custom development of strip detectors for private companies:

- single/double-side,
- DC/AC coupled,
- punch-through biasing
- very low leakage,
- high yield

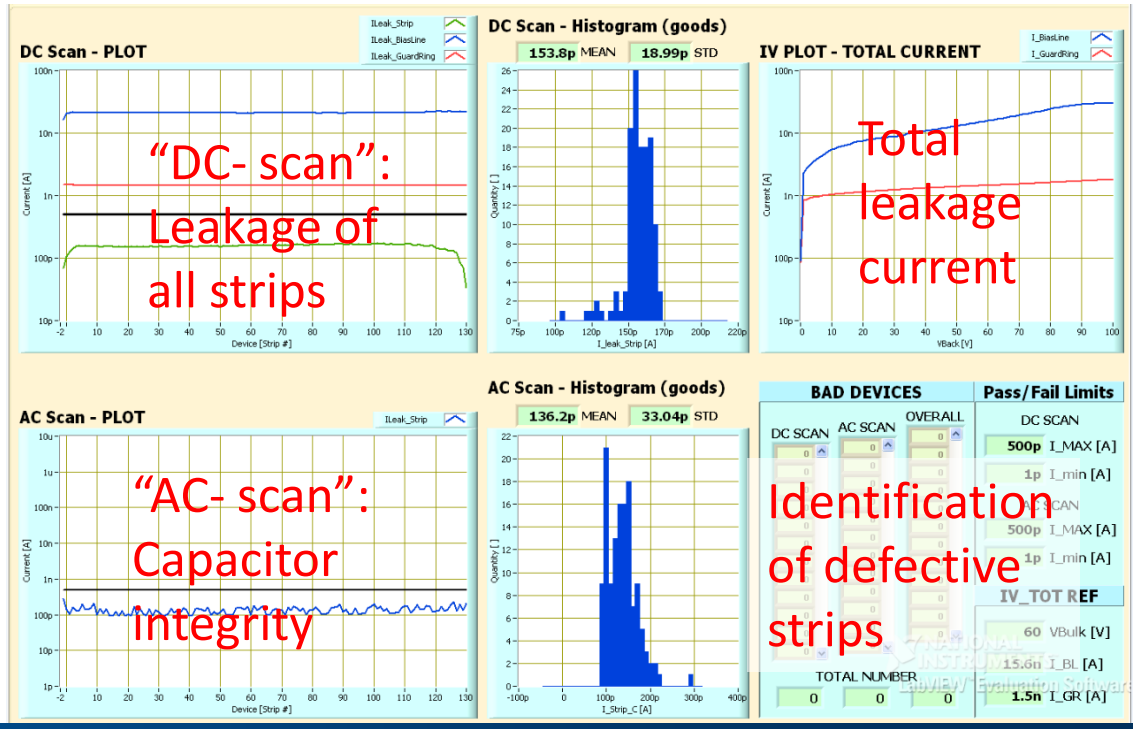

Strip Detectors: examples

AMS experiment (@ISS)

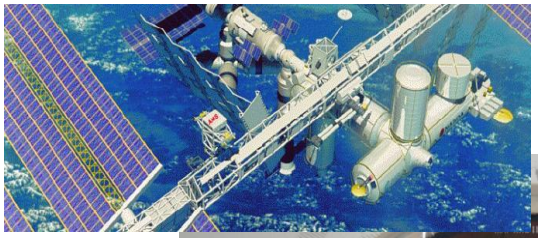

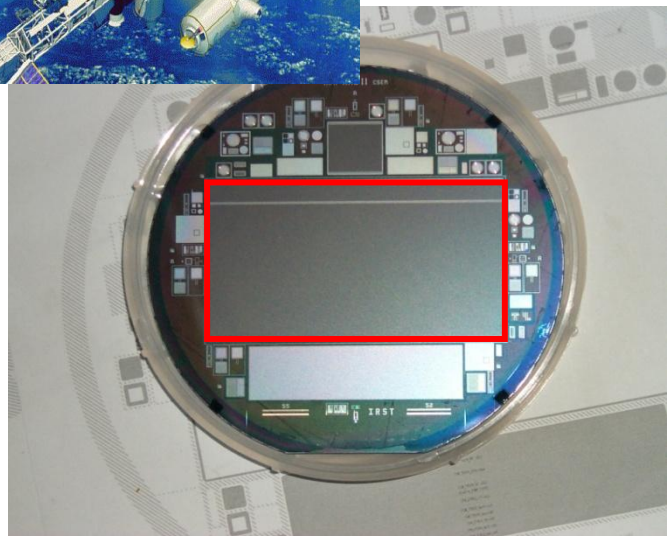

Silicon microstrip detectors:

700 large-area double-sided in spec detectors fabricated in 2002-2004.

ALICE experiment (@LHC)

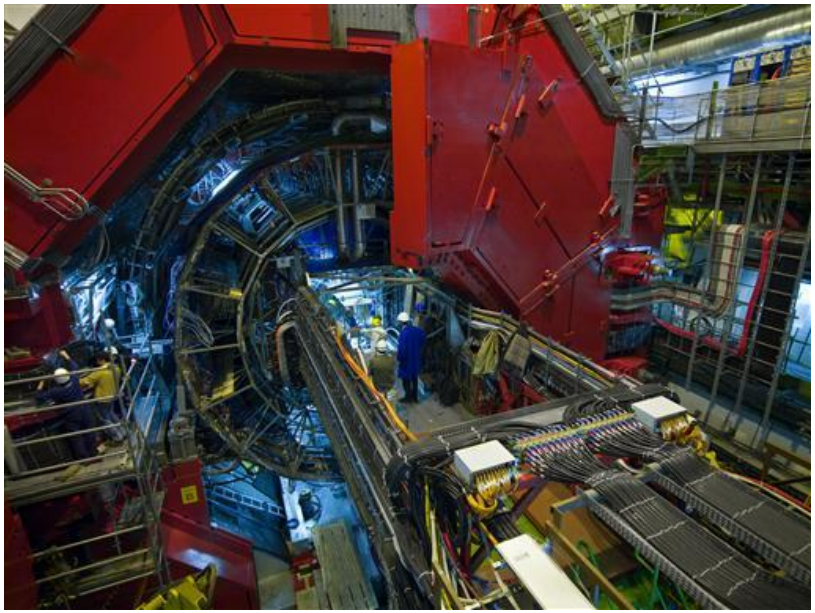

Silicon microstrip detectors:

600 large-area double-sided in spec detectors fabricated in 2003-2005.

ALICE Industrial Awards in 2006

The ALICE microstrip detector

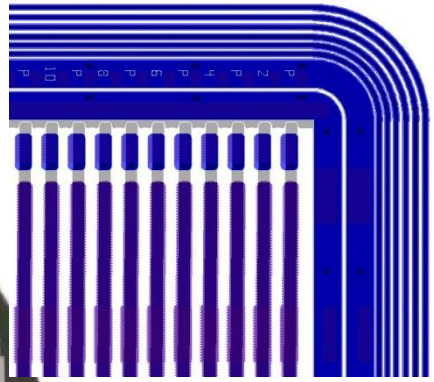

- Double-sided strip detector
- AC-coupled strips (integrated capacitor)
- Punch-Through biasing on both sides
- p-stop isolation at the n-side
- Overall size: 75mm X 42mm
- 768 strips on each side
  - 40mm long
  - 95µm pitch
  - 35mrad stereo angle

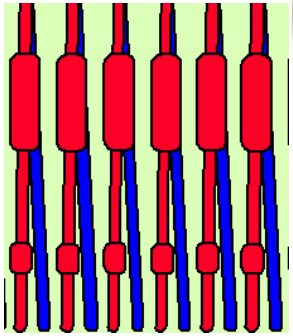

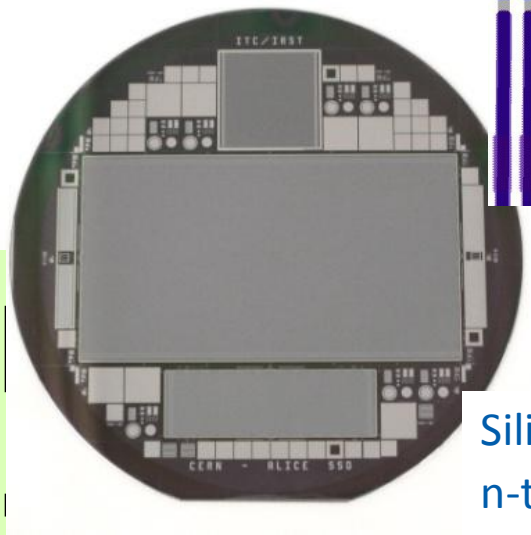

Silicon substrates: n-type , FZ, <111>, V_{depl} < 50V

Detector selection criteria and measured values

Parameter	threshold	Typical values
Total detector current @ 60V	< 7µA	< 500nA
single strip leakage current @ 60V	< 20nA	< 750pA
coupling capacitor leakage current @ 20V	< 1nA	< 50pA
# of defective strips/detector	< 30	<5

Detector leakage current

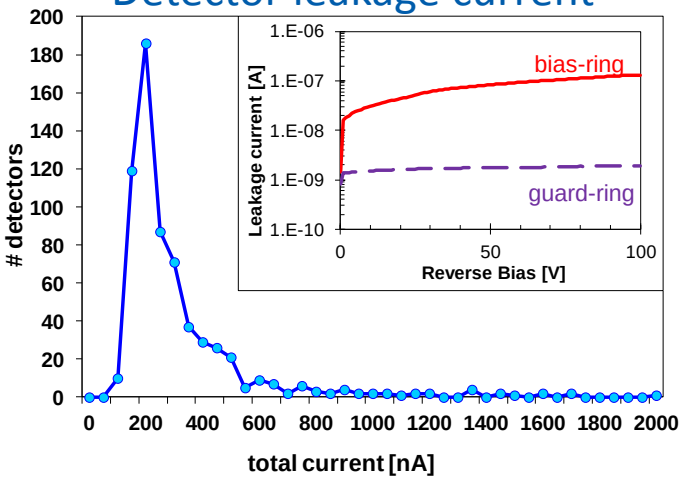

FBK 3D technology

Double side fabrication process

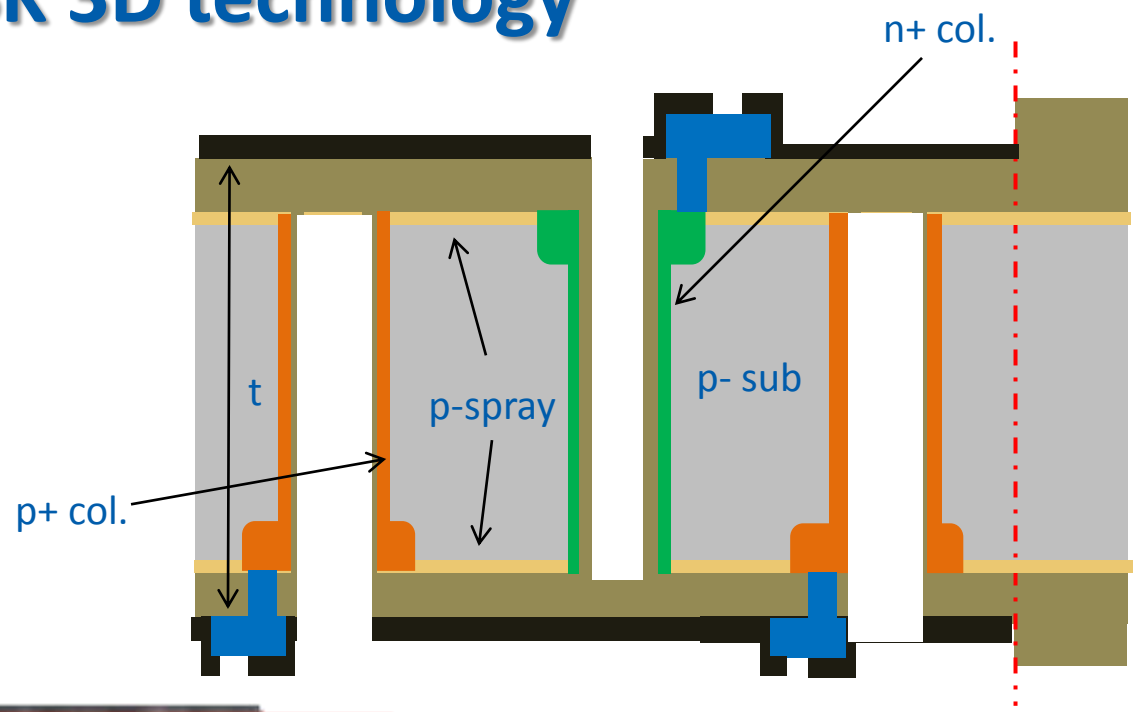

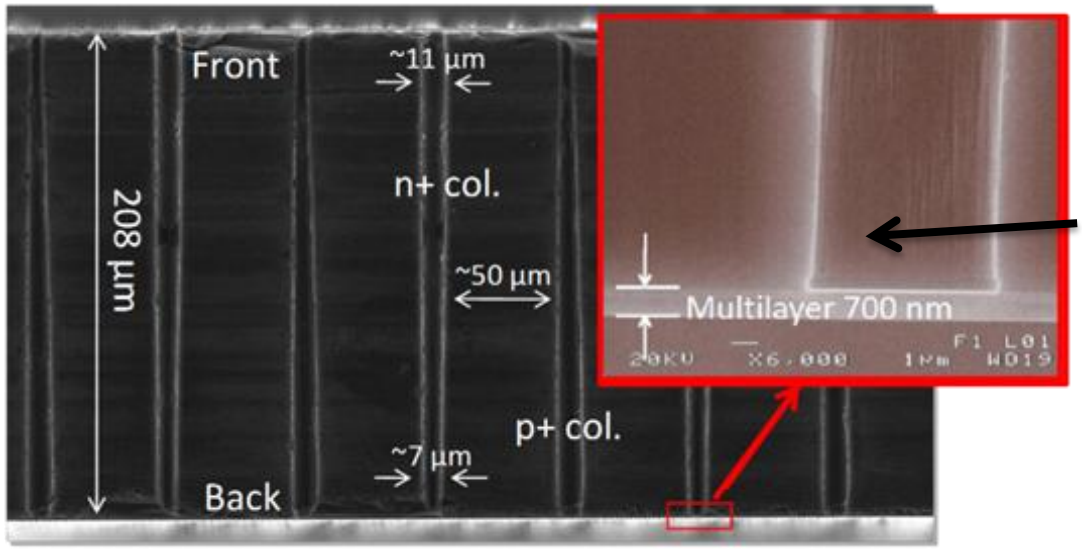

Empty column

- p-implanted silicon
- n-diffused silicon
- p-diffused silicon
- Aluminum metal
- dielectric
- silicon
- PECVD overglass

Active edge

- 4.5µm wide trench
- 200µm deep
- polysilicon filled

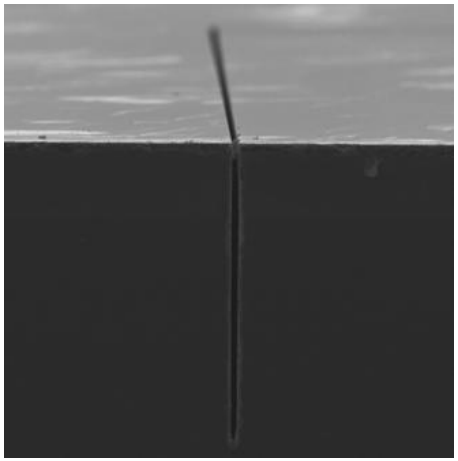

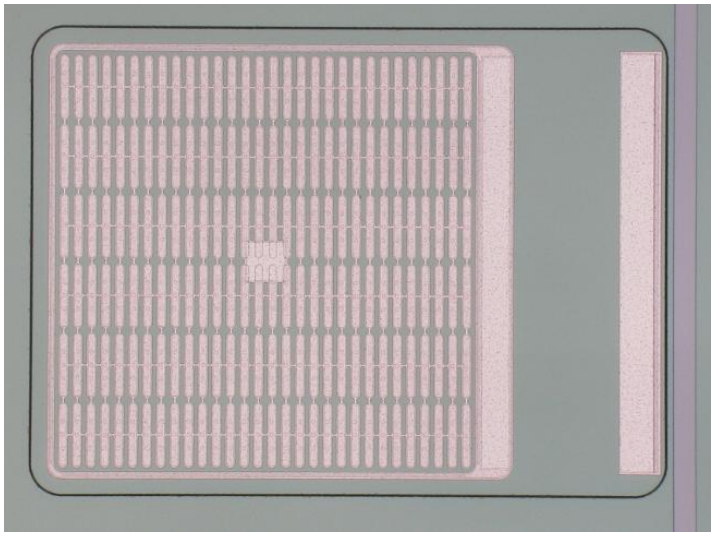

INFN-BA, CERN

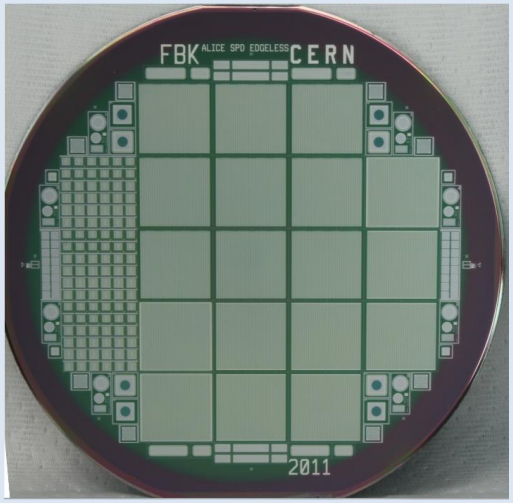

2 running projects:

- pixel sensors compatible with ALICE ROC (epi wafers, 100µm thick + sub)

- pixel sensors compatible with ATLAS FE-I4 (200µm-thick FZ + waf-bond sub)

LPNHE Paris

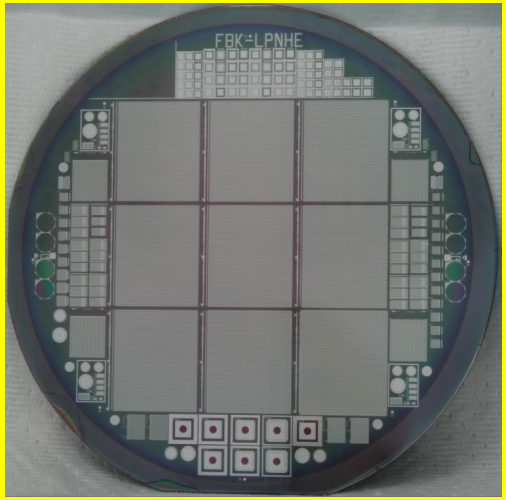

Silicon Drift Detectors

2 public project:

- INFN/INAF (2011-)
  development of very large
  linear SDD for astrophysics experiment

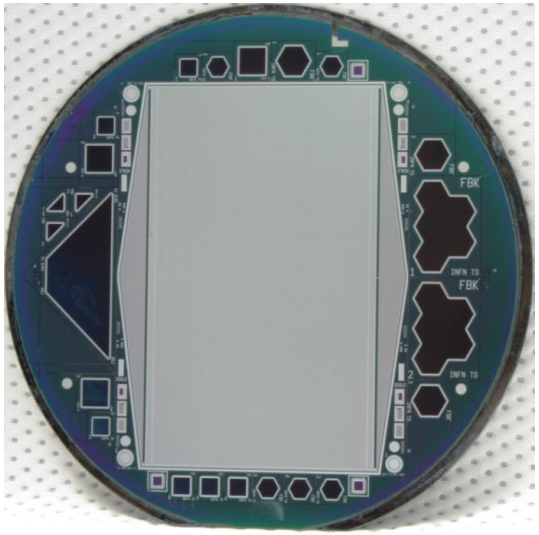

- ESA - PoliMi (2010-2012)
  development of gamma ray spectrometer
  based on SDD coupled to $LaBr_3$ scintillator

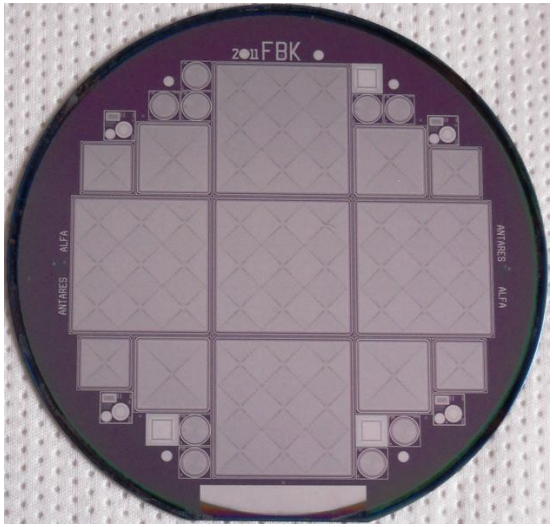

SDD ESA
Read-out of $LaBr_3$ scintillator

ARC as passivation on the back

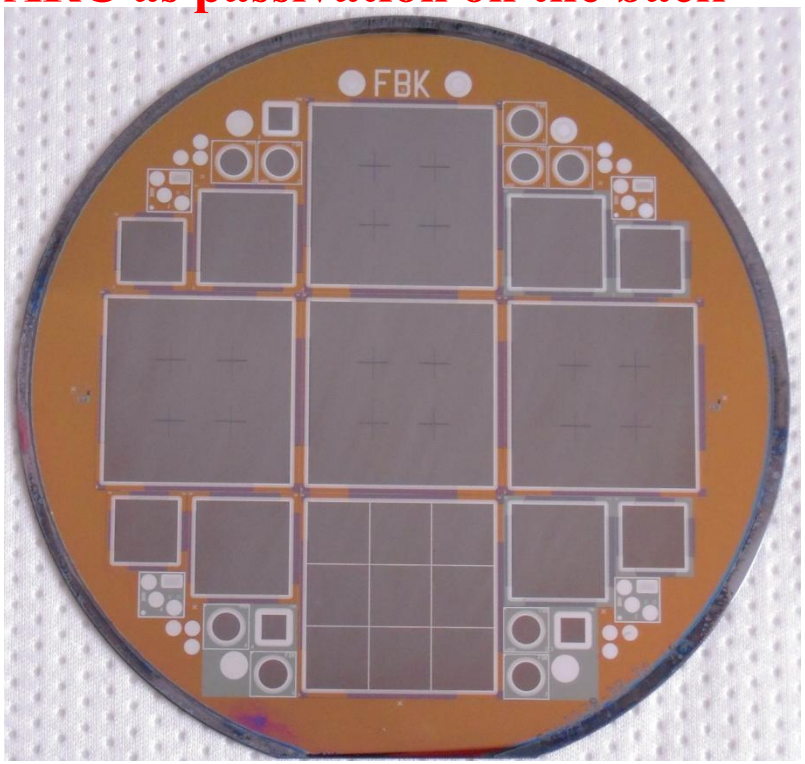

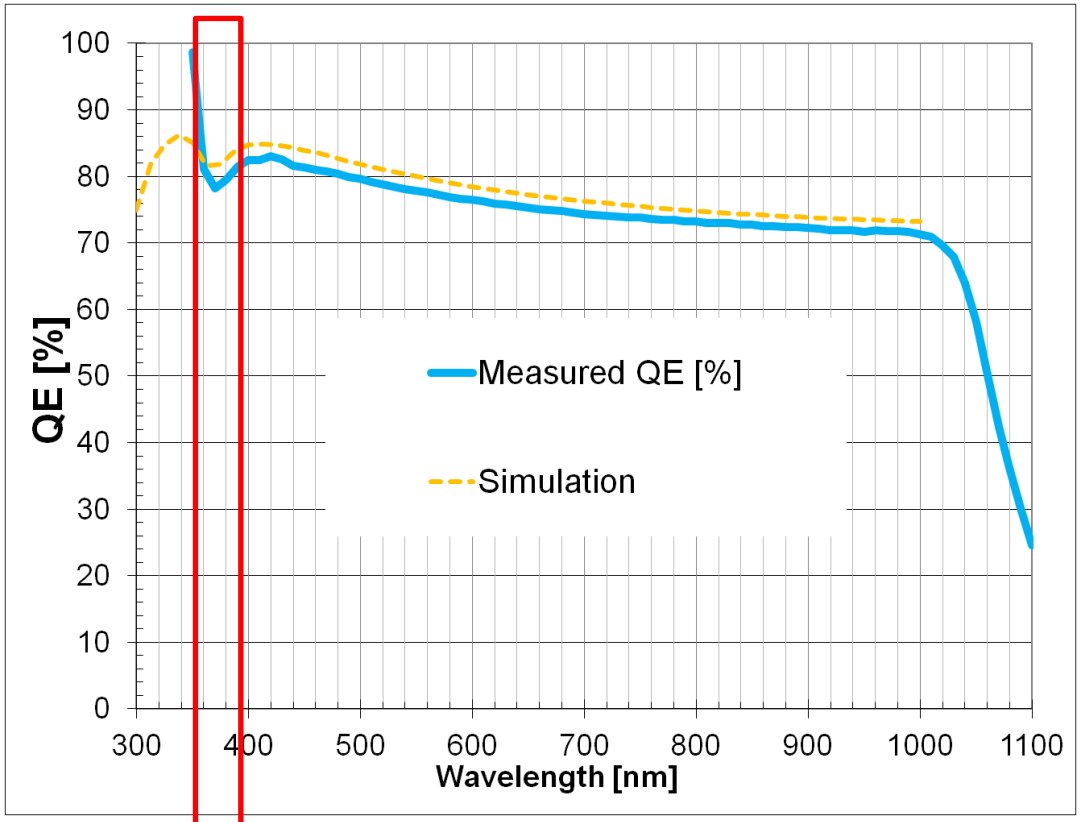

Emission range of LaBr3: 360-380 nm (NUV)

Silicon Drift Detectors

gamma spectrometer for ESA

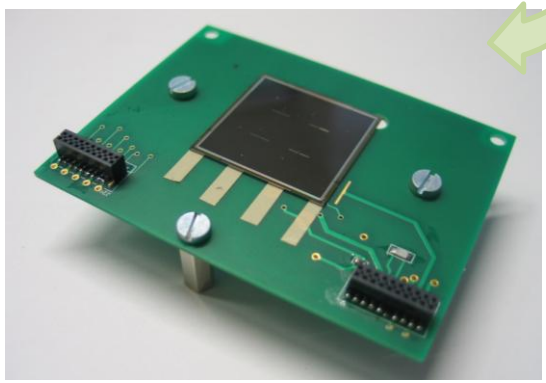

T=: -20°C
peaking time: 6 µs

^{57}Co, ^{137}Cs, ^{60}Co spectra measured with the SDD array coupled to a 1'' $LaBr_3$ crystal

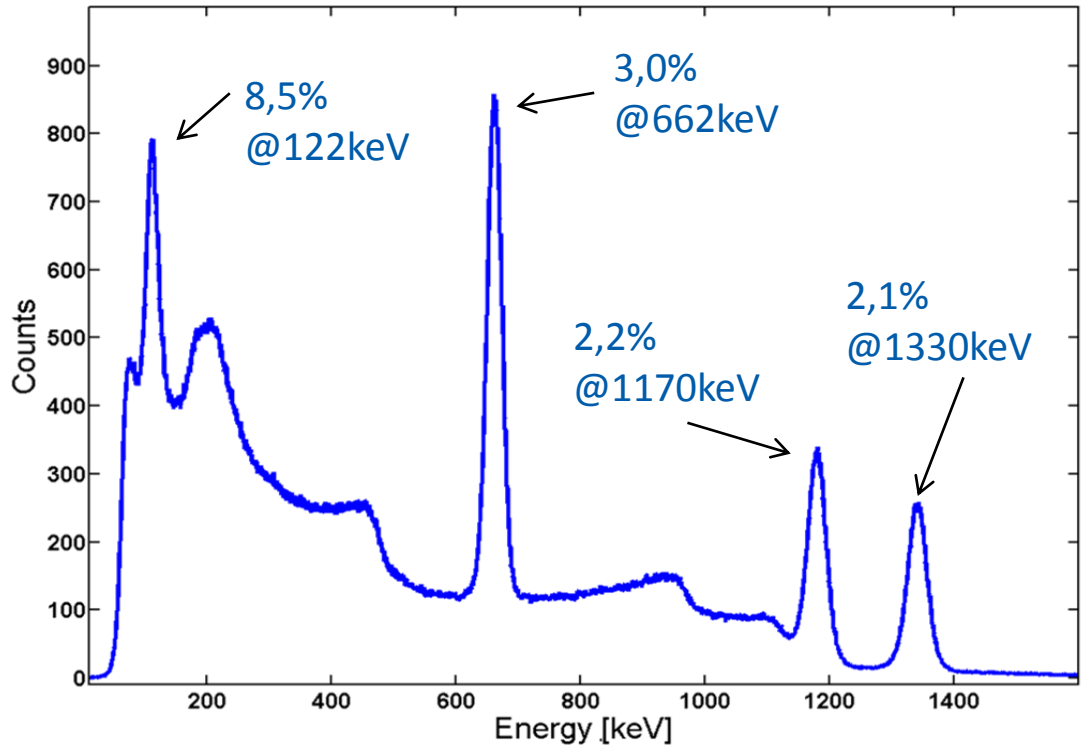

(Energy resolution @662keV measured with a PMT = 3.2%)
(courtesy F.Quarati)

C. Fiorini et al., "Silicon Drift Detectors for Readout of Scintillators in Gamma-Ray Spectroscopy", IEEE TNS, VOL. 60, NO. 4, AUGUST 2013 2923

Silicon photomultiplier

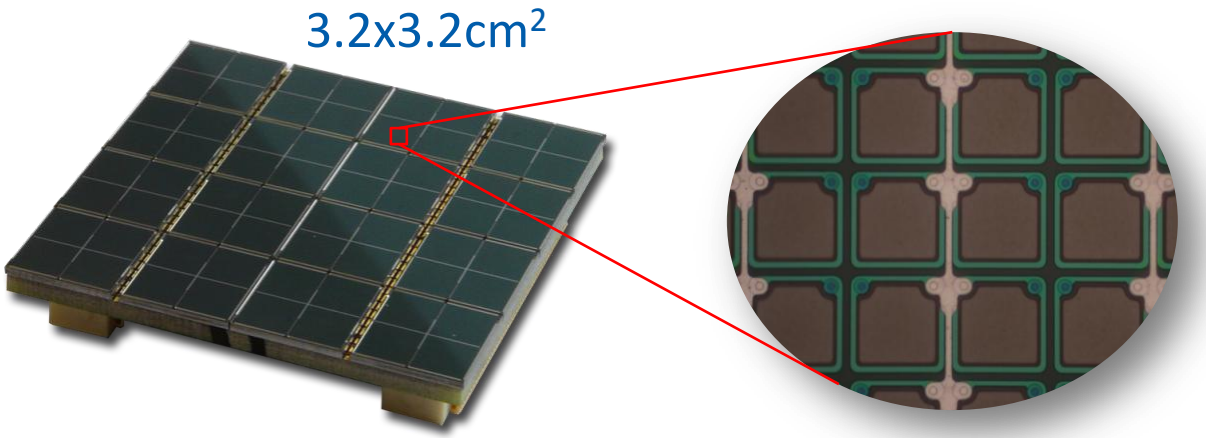

SiPM

array of tiny SPADs connected in parallel to give proportional information

Main Current Projects

EU projects:

- Sublima (2010 – 2014)
- Insert (2014 - …)

National projects:

- with INFN (2013-2015)

Application fields:

detection of faint light with high time resolving capability:

- nuclear medicine
- biology
- physics experiments
- instrumentation for material analysis

FBK technology evolution

FONDAZIONE BRUNO KESSLER

Original technology 2006

2010-11

RGB-SiPM
(Red-Green-Blue SiPM)

- excellent breakdown voltage uniformity
- low breakdown voltage temperature dependence
- higher efficiency
- lower noise

electric field engineering

2012

NUV-SiPM
(Near-UV SiPM)

new junction

- excellent breakdown voltage uniformity
- low breakdown voltage temperature dependence
- high efficiency in the near-ultraviolet
- very low dark noise

2012

RGB-SiPM_HD
(Red-Green-Blue SiPM – high density)

new cell border

- small cell size with high fill factor:
  - high dynamic range
  - low excess noise factor

FBK Technologies and main features

	Original n+/p	RGB-SiPM (Upgraded n+/p)		NUV-SiPM
			HD	
Breakdown voltage	33V	28V	28	26V
Breakdown voltage uniformity on wafer	~3V	**<0.2V**	**<0.2V**	**<0.2V**
Max over-voltage	~8V	~6V	~8V	~5V
V_{BD} temp. coeff.	75mV/C	**25mV/C**	**25mV/C**	**25mV/C**
Max primary dark rate (20C)	several MHz/mm^2	~500kHz/mm^2	~1MHz/mm^2	**~150kHz/mm^2**
Peak PDE	450-600nm	450-600nm	450-600nm	**390nm**
Wavelength range	300-900	300-900	300-900	300-600
Peak PDE	25%	33%	28%	32%
ECF (at max PDE)	1.5	1.8	**1.1**	2
	50um cell 45% FF	50um cell 45% FF	**15um cell 45% FF**	50um cell 45% FF

Outline

- silicon sensor activity in FBK
- excess noise in silicon microstrip detectors:
  - $ENC^2 \sim sqrt(\tau)$
  - $ENC^2 \sim I^2_{PT}\,\tau^2$
  - thermal noise

ALICE μ-strip detectors:

n-side insulation methods

FBK: 3 *p*-stops

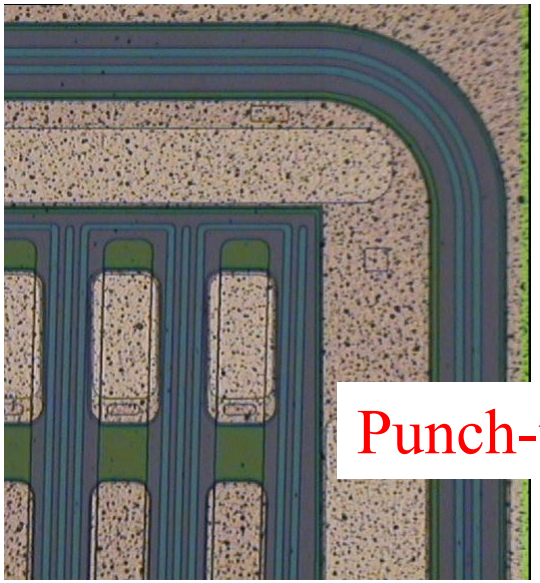

Canberra: *p*-spray

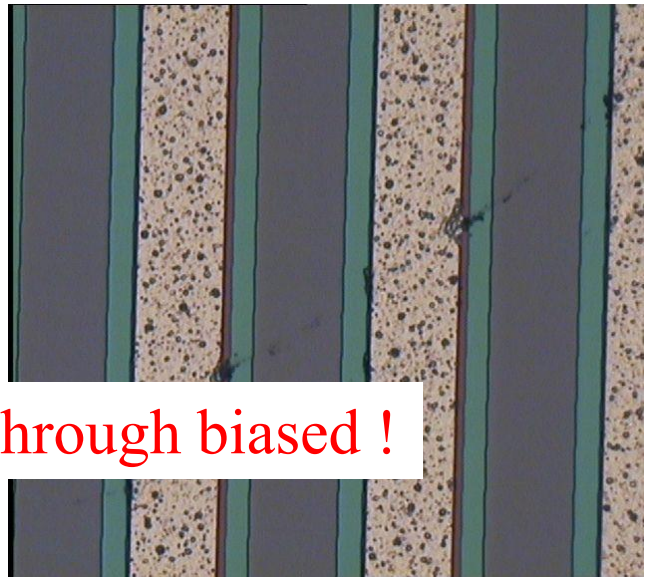

Sintef: 2 *p*-stops

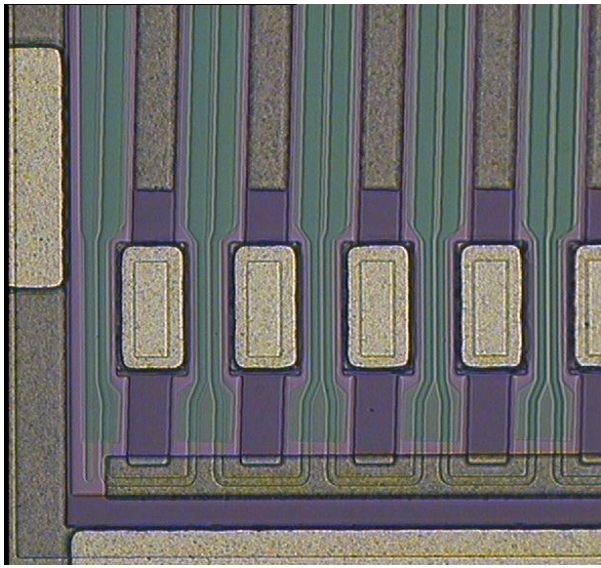

Punch-through biased !

CANBERRA

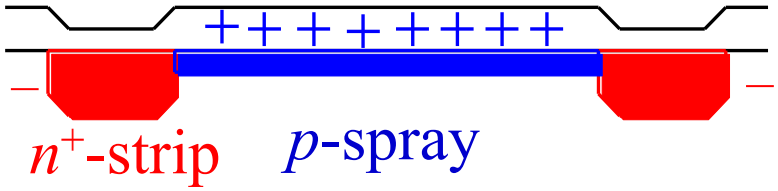

FBK/SINTEF

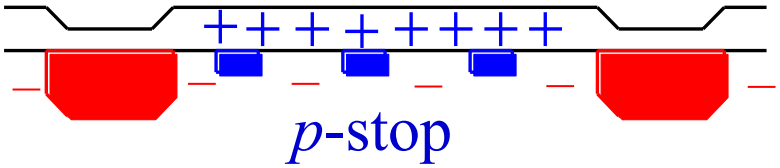

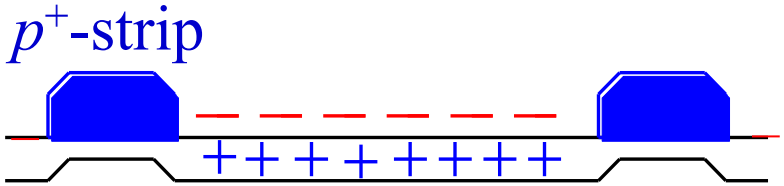

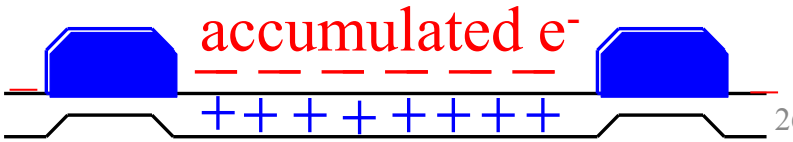

FONDAZIONE BRUNO KESSLER

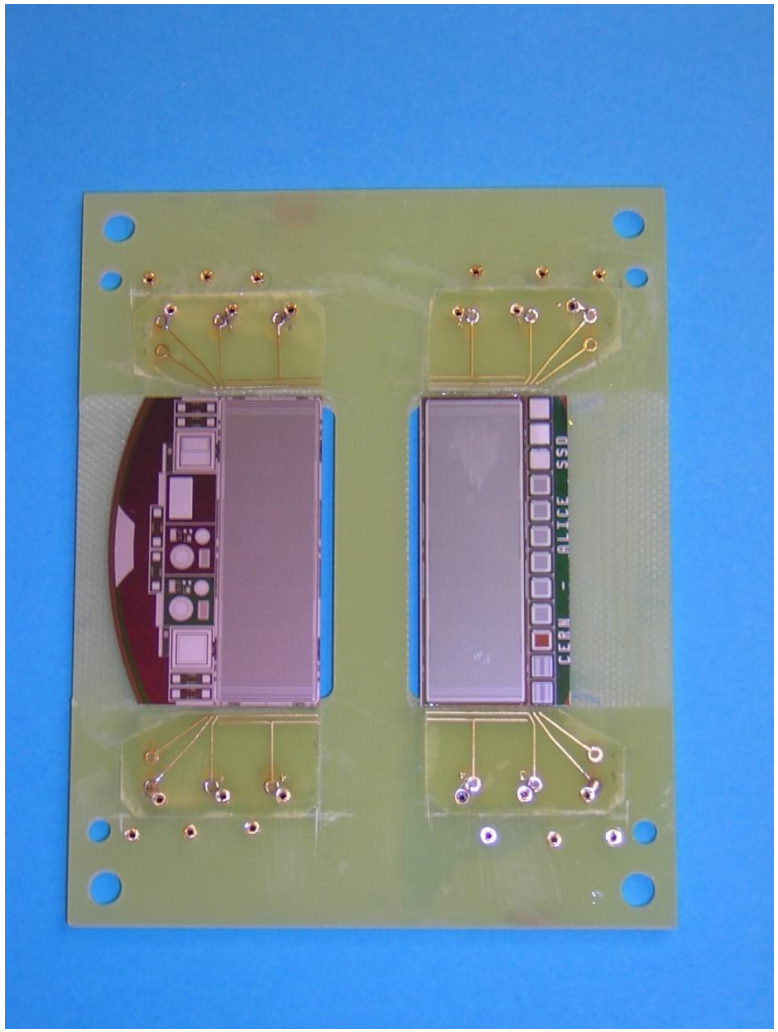

For each detector, for each side (n- and p-), the following terminal are connected to a separate line::

- the AC pad of one strip
- the DC pad of the same strip
- the AC pads of all the other strips
- the Bias Ring

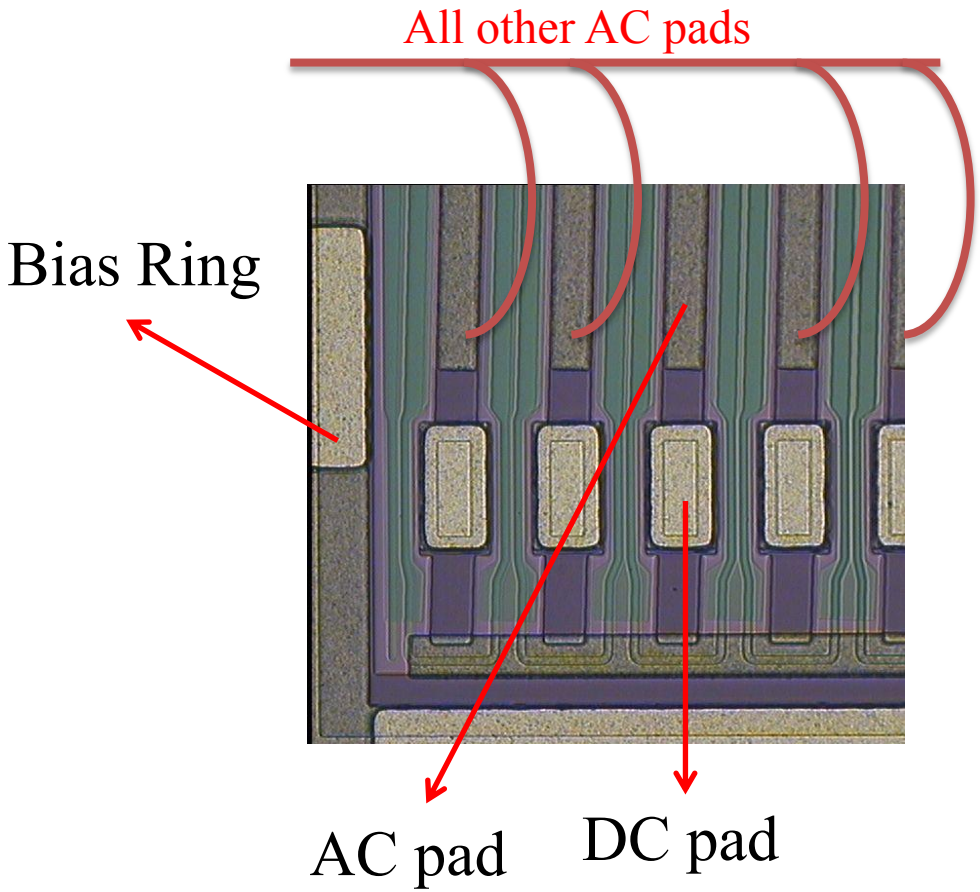

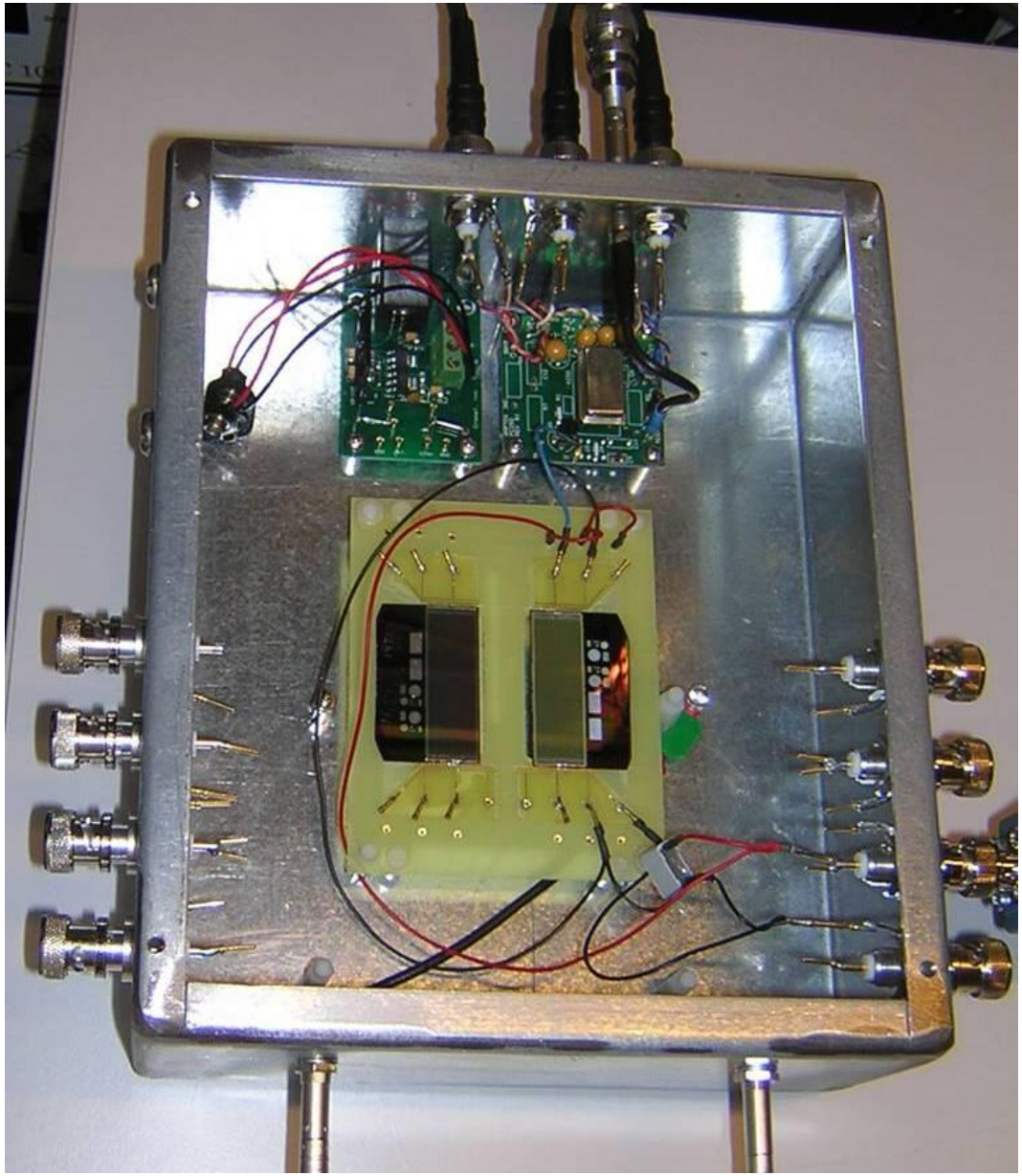

Measurement set-up

Detector and front-end amplifier
are inside a shielding box.

Measurement set-up: closer view

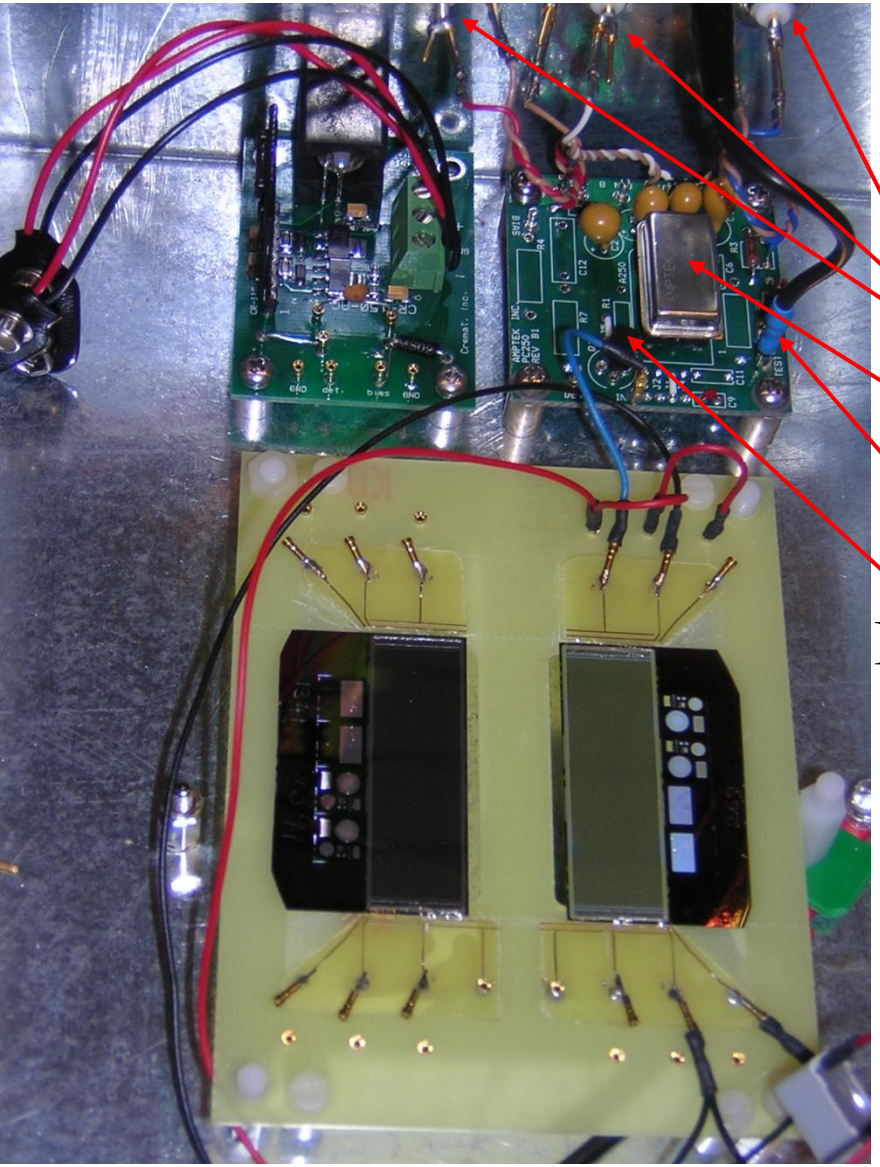

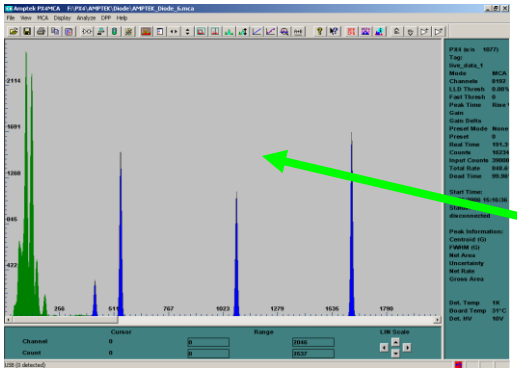

Amptek PX4 Digital Shaper

BNC connectors

A250 pre-amp

Test input cable

Input FET

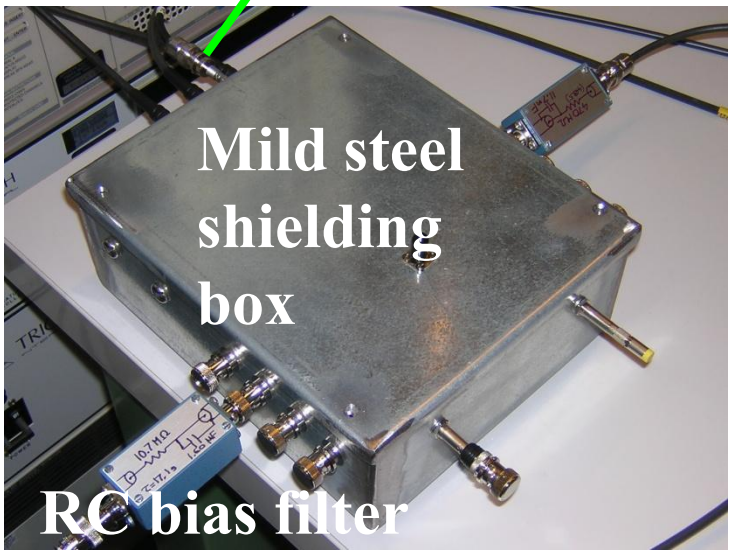

Mild steel shielding box

RC bias filter

ALICE μ-strip detectors

Alternative biasing methods

Since the DC pad is contacted, several biasing methods of the strip under test are possible.

Strip biasing with an external resistor

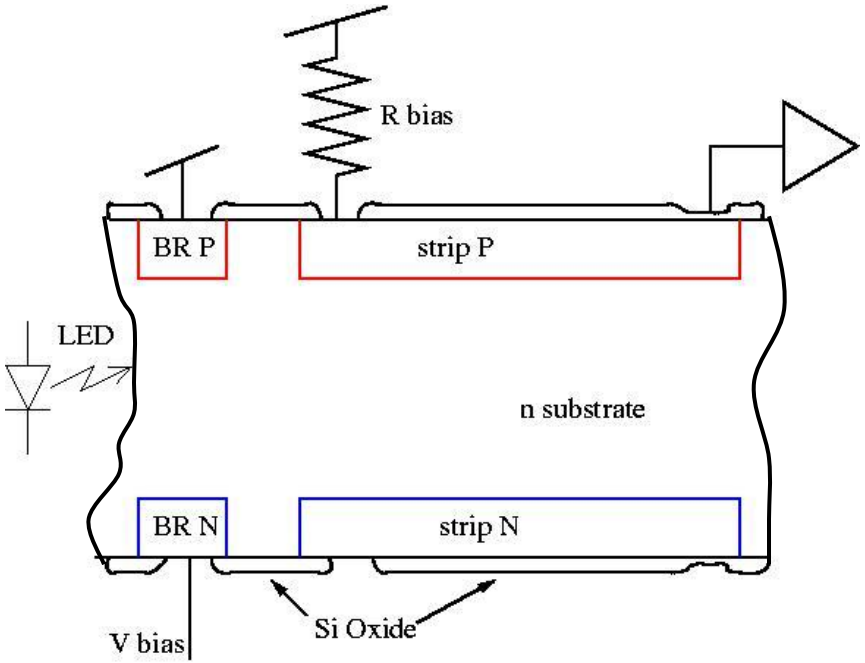

No punch-trough current flows

Current injection through an external resistor

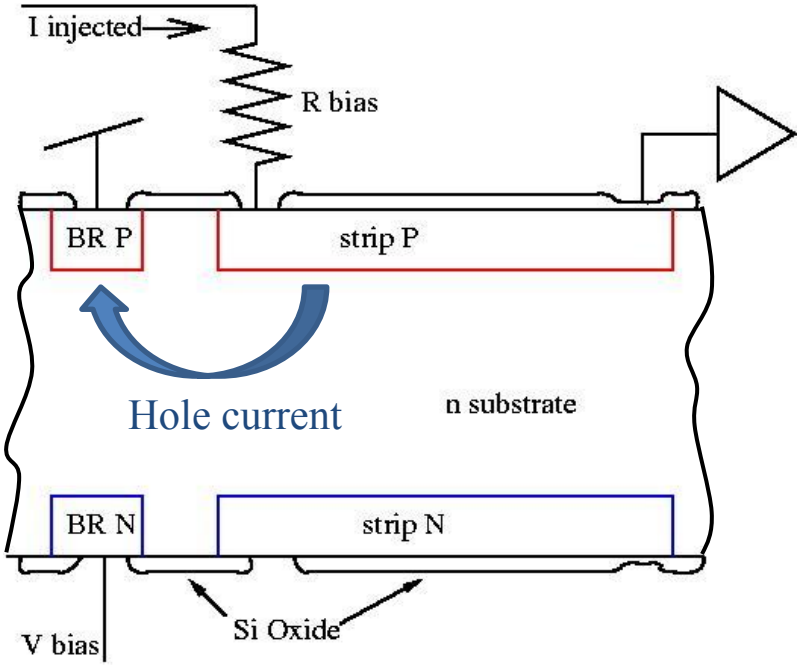

The punch-trough current is the sum of leakage current and injected current

Noise measurements on ALICE μstrips

The noise model has been verified on every detector.
In particular some points have been caught:

- The punch-trough current contributes to shot noise

  $\Longrightarrow$ in AC set up the leakage current gives a noise contribution $4q\, I_{\mathrm{Leakage}}$

- Injection of current trough a resistor does not contribute to noise

ENC vs. peaking time for various leakage currents

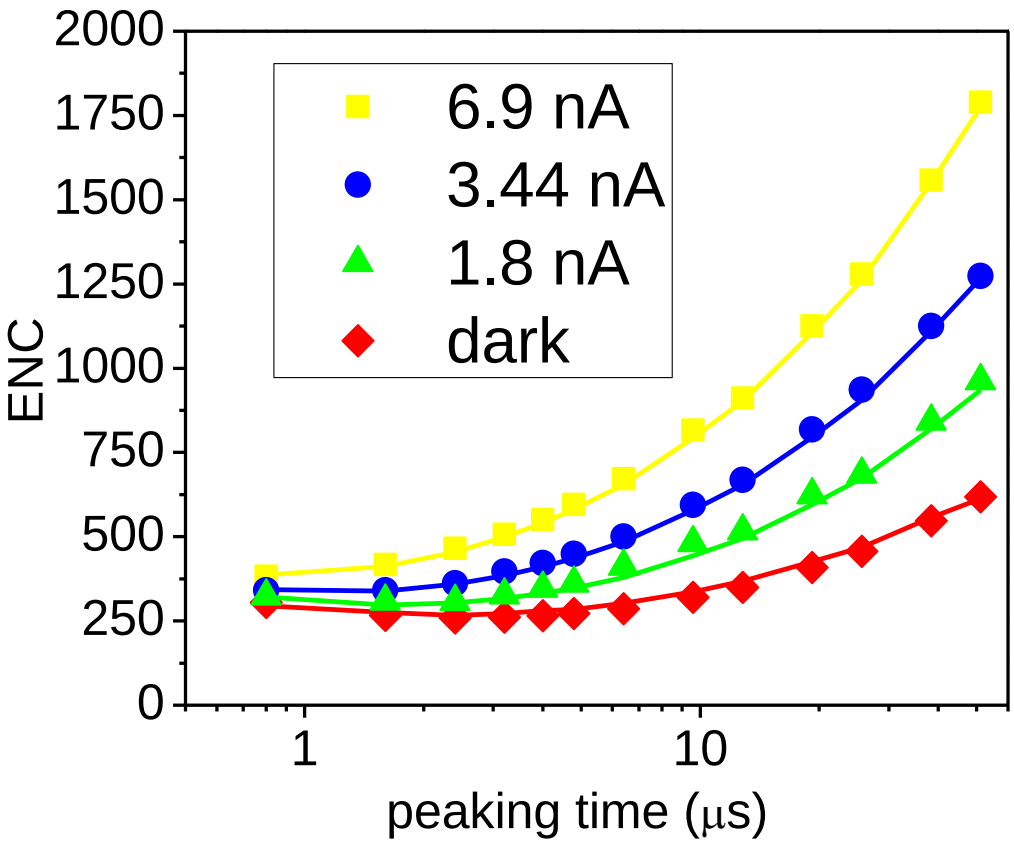

The experimental data points are shown together with the expected theoretical curves.

$ENC^2 = A_1\tau + A_2\, C^2_{in}/\tau + A_3 C^2_{in}$

→ OK !

Measurements were made for every kind of polarization and for both *n* and *p* side.

Canberra P side (50V)

Noise versus V_{bias}

We varied τ, $I_{leakage}$, polarization methods.
Changing the V_{bias} is not expected to make a significant difference.
For voltages just above depletion, the measured noise is higher than predicted by the model.

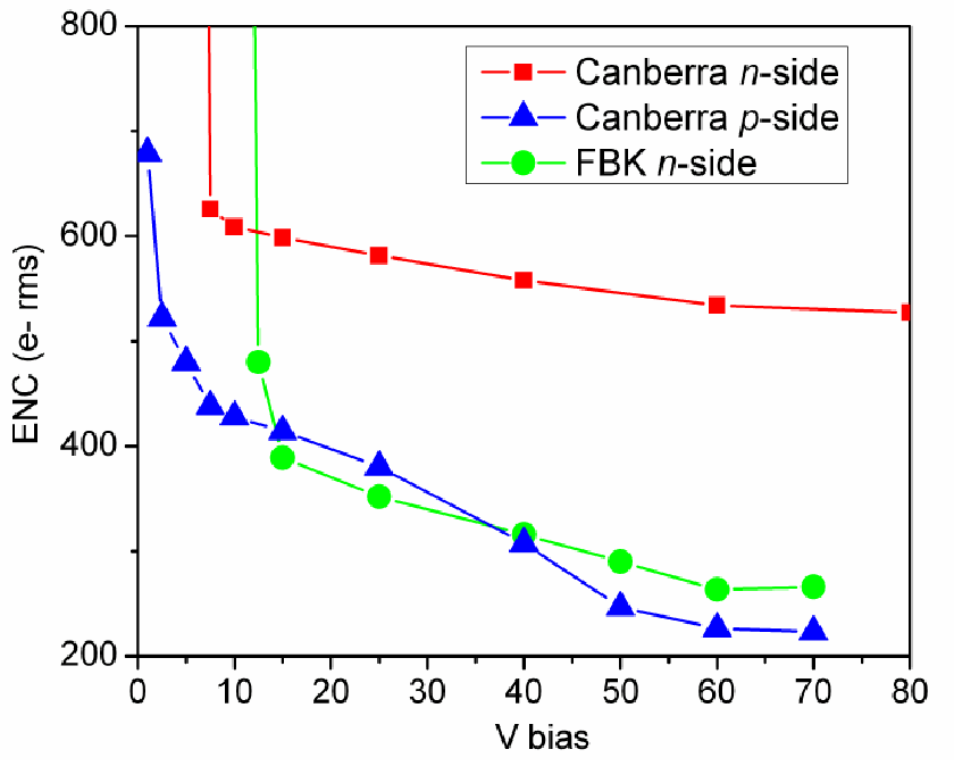

Excess noise on Canberra and FBK sensors

-> For low voltages on Canberra p-side and FBK n-side
-> For every bias on Canberra n-side
strips exhibit an unexpected excess noise, which is:

- independent of the current
- $(ENC)^2 \propto \sqrt{\tau}$

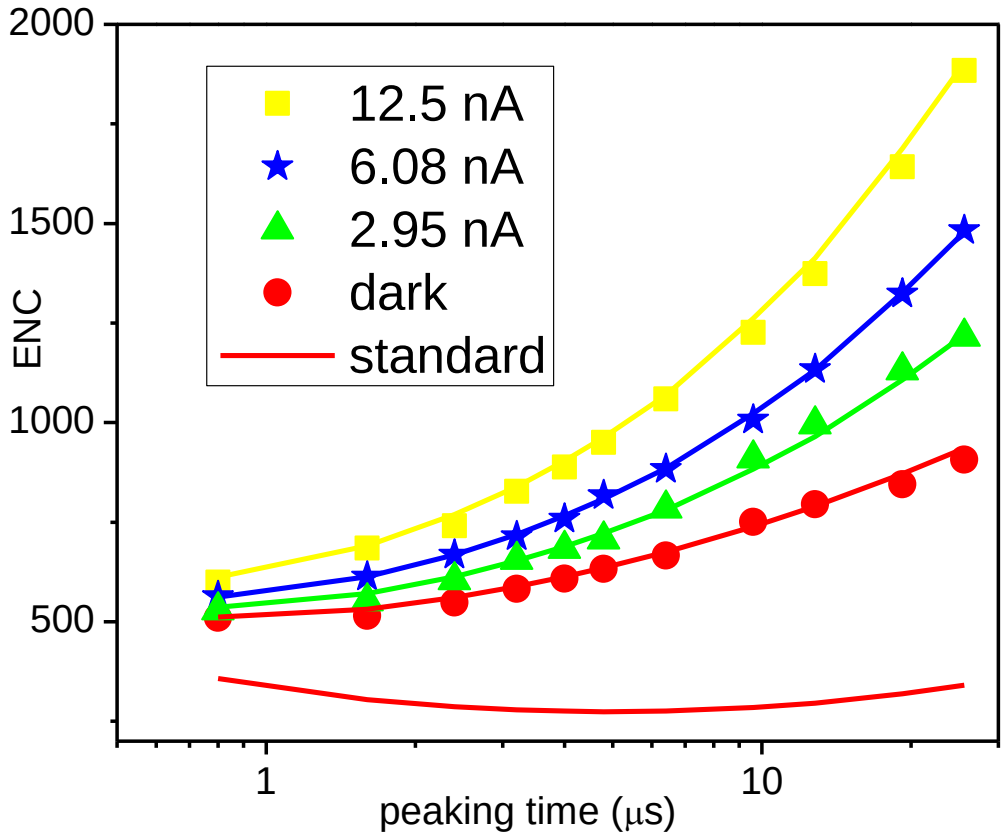

Canberra n-side

A step back:

Admittance measurements on μ-strip

$$Y = G + i\,\omega\,Cp \;,\; D = Re(Y) / Im(Y)$$

AC pad @ LOW

Bias Ring @ GND

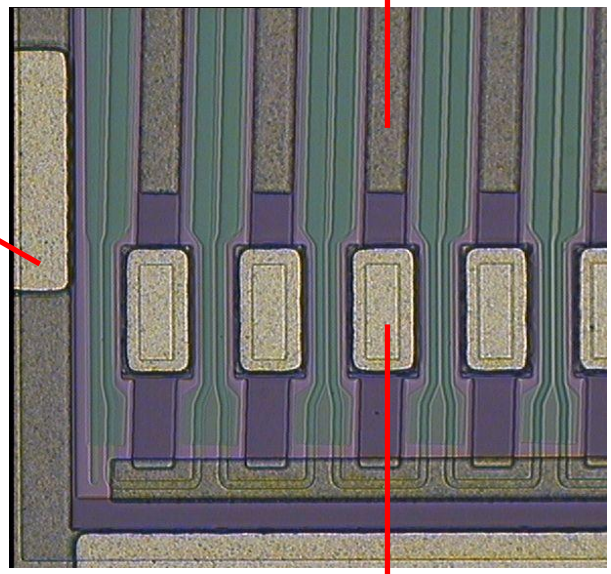

Back @ V
(GND in AC)

DC pad floating

G. Giacomini, , L. Bosisio, I. Rashevskaya, O. Starodubtsev,
"Study of frequency-dependent strip admittance in silicon microstrip detectors",
NIM A, 624 (2010) 344–349

Strip capacitance measurements: **Y vs V_{bias}**

- On Canberra n - side, D is constant and high for every V_{bias}.
- On Canberra p - side and FBK n-side, D decreases with V_{bias} and flattens above 50 – 60 V

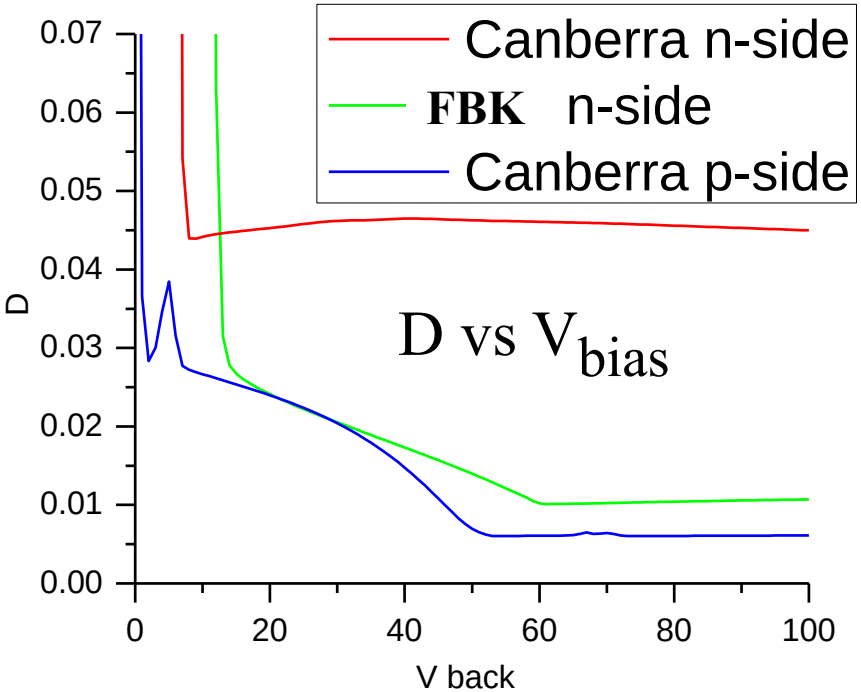

What is common between
Canberra *n*-side and
Canberra *p*-side or FBK n-side (at low voltages)?
Canberra *n*-side strips are insulated by a resistive *p*-spray implant (never gets depleted).
Resistive layers exist also on the other two: accumulation electrons under the oxide, that may deplete at high enough bias voltage.

D and C_p vs frequency on Canberra

Solving the simple circuit representing Canberra (both sides), we can reproduce the measured C and D dependence on frequency.

At high V_{bias} the accumulation layer vanishes ($R \rightarrow \infty$) $\Rightarrow$ *C, D* independent of *f*

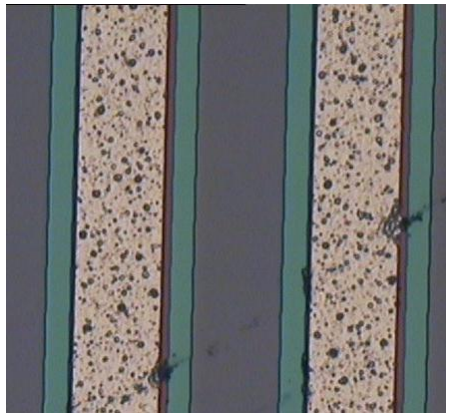

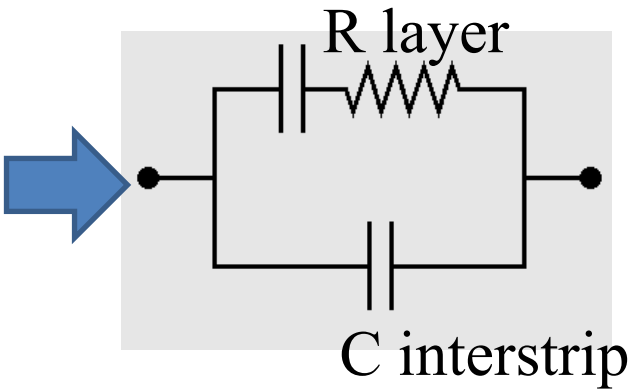

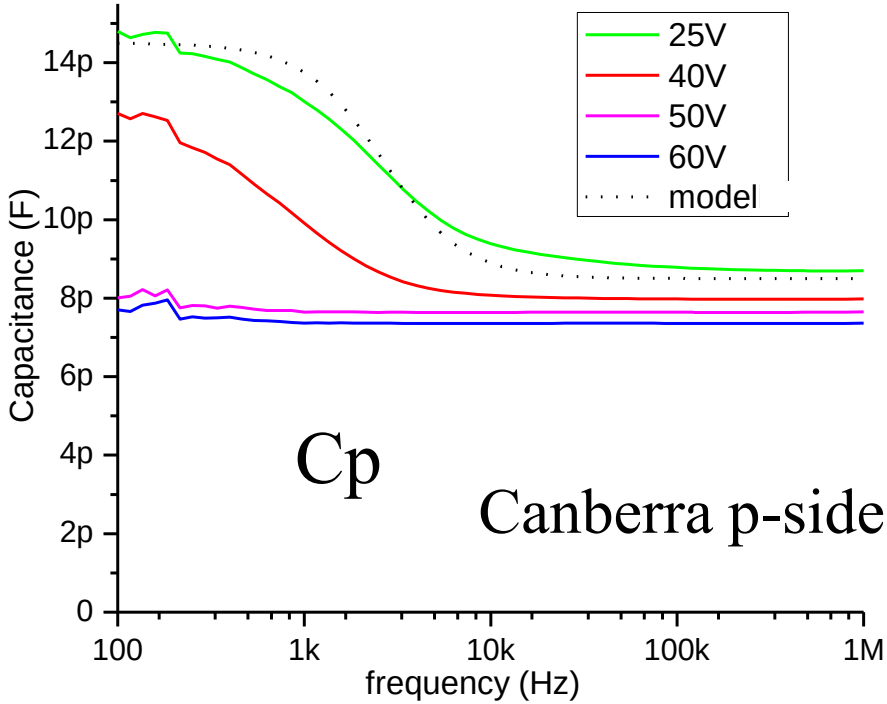

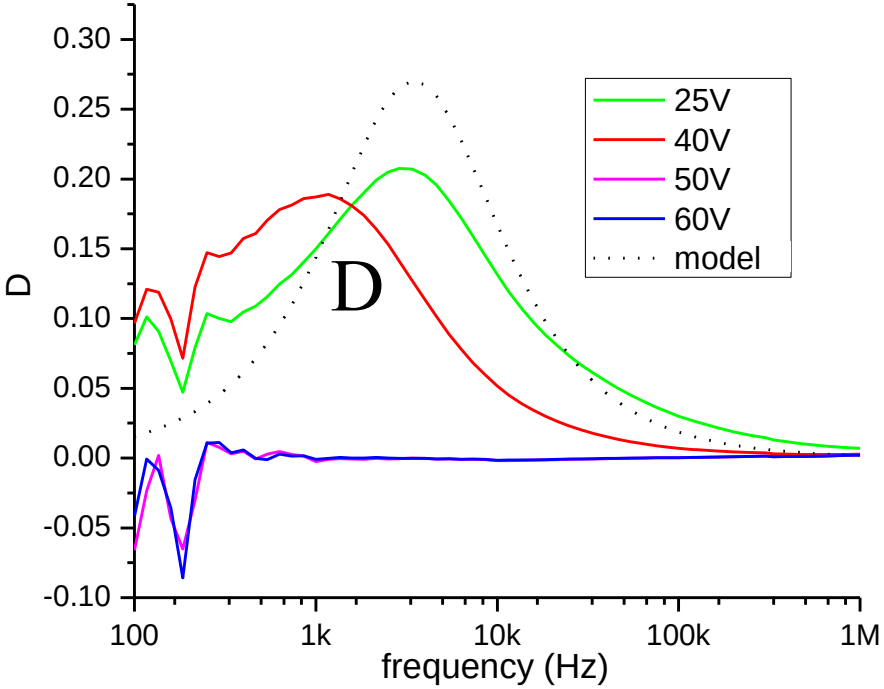

D and C_p vs frequency on FBK n-side (p-stop insulation)

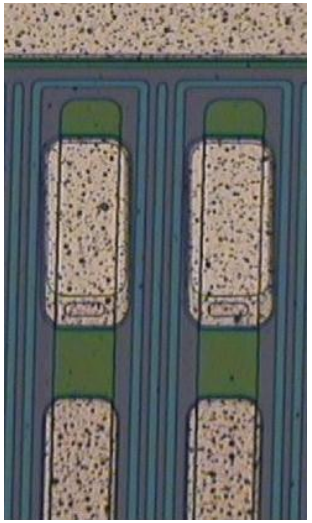

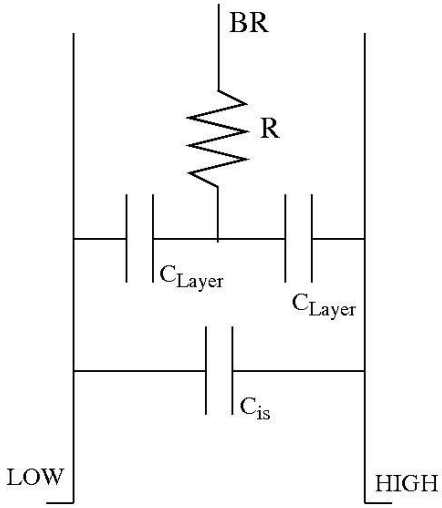

At high V_{bias} the accumulation layer vanishes (R → ∞) ⇒ *C, D* independent of *f*

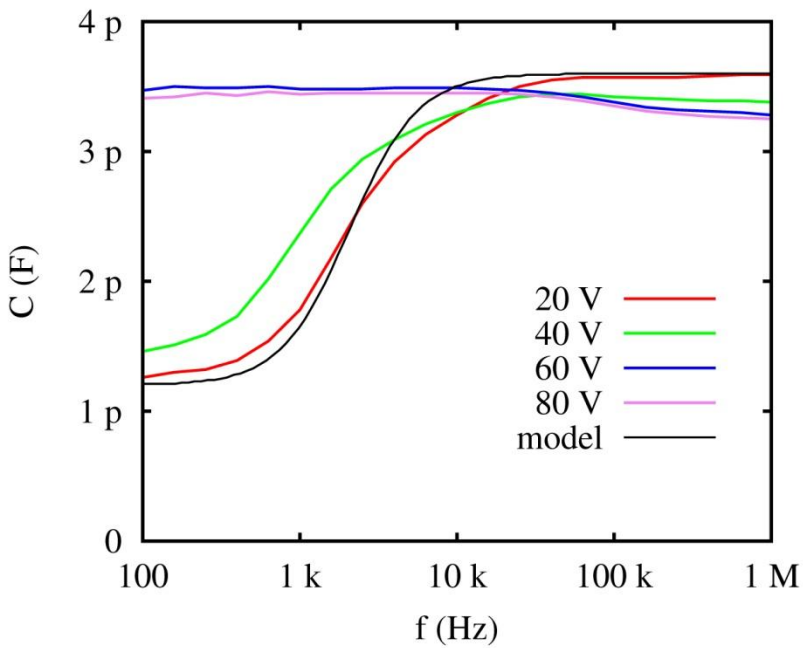

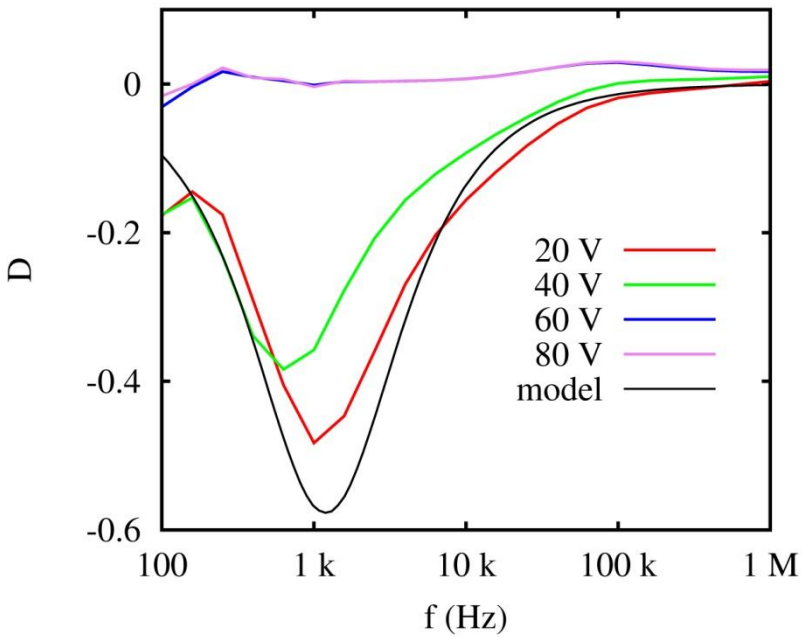

3D simulations

Numerical 3D simulations with ISE-TCAD software confirm the interpretation:
The narrow region between strips and bias ring depletes from **electrons**
The bias V at which this occurs is strongly dependent on Q_{oxide}
(ranging from 1 to 5×10^{11} q/cm^2)

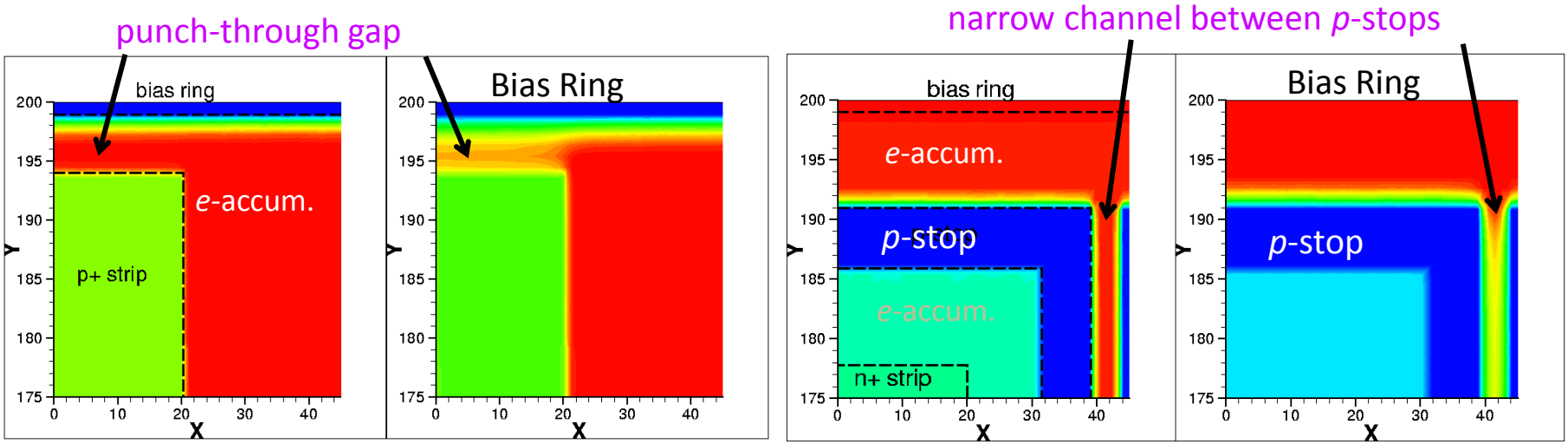

Lower V_{bias} *Continuous* | Higher V_{bias} *Interrupted*

<---------- Canberra *p*-side ----------->

Lower V_{bias} *Continuous* | Higher V_{bias} *Interrupted*

<---------- FBK *n*-side ---------->

Noise versus V_{bias}

Canberra p-side

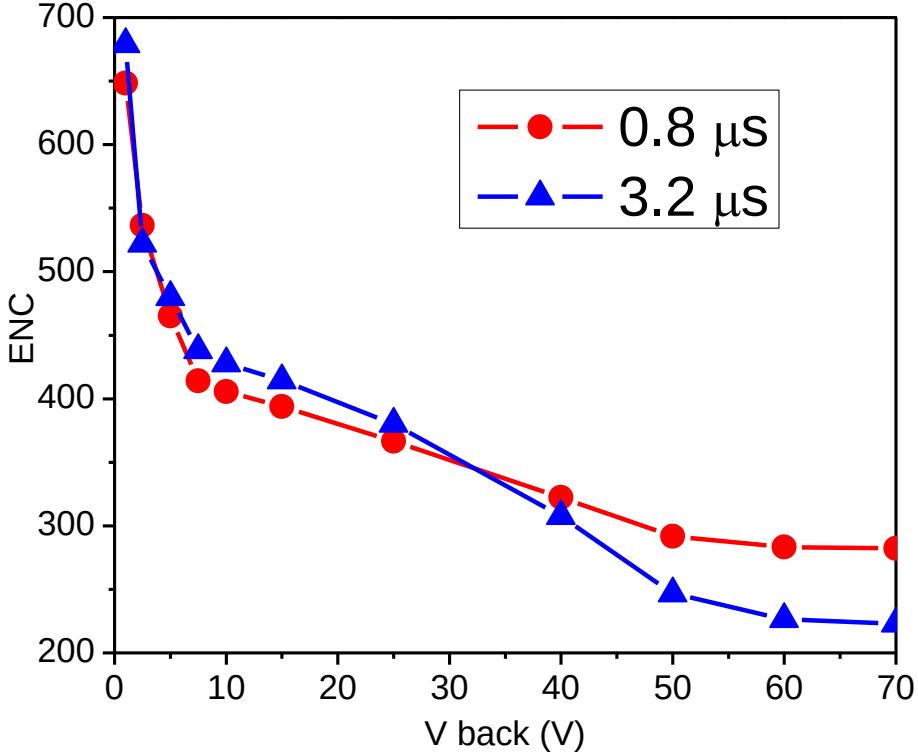

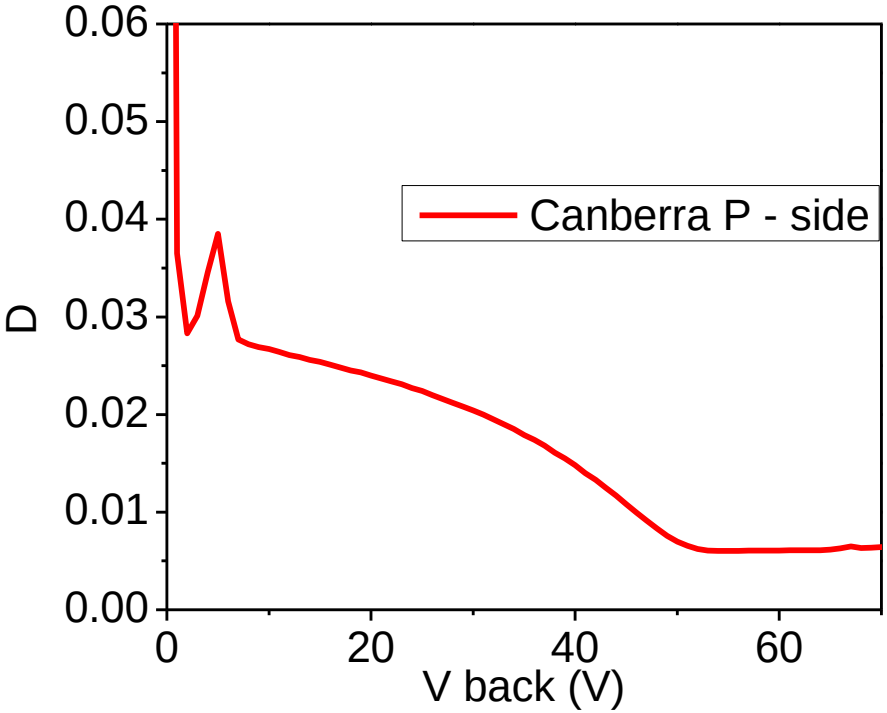

<u>Continous Resistive paths at the Si-SiO_2 interface are responsible for this excess noise.</u>

G. Giacomini, L. Bosisio, I. Rashevskaya, and O. Starodubtsev,
"Noise Characterization of Double-Sided Silicon Microstrip Detectors With Punch-Through Biasing",
IEEE TNS VOL. 58, NO. 2, 2011, pag. 569

Outline

- silicon sensor activity in FBK
- excess noise in silicon microstrip detectors:
  - $ENC^2 \sim sqrt(\tau)$
  - $ENC^2 \sim I^2_{PT}\,\tau^2$
  - thermal noise

Excess noise in Sintef sensors

Sintef *p*-side shows a contribution to $(ENC)^2 \sim (I_{punch\text{-}through})^2 \tau^2$

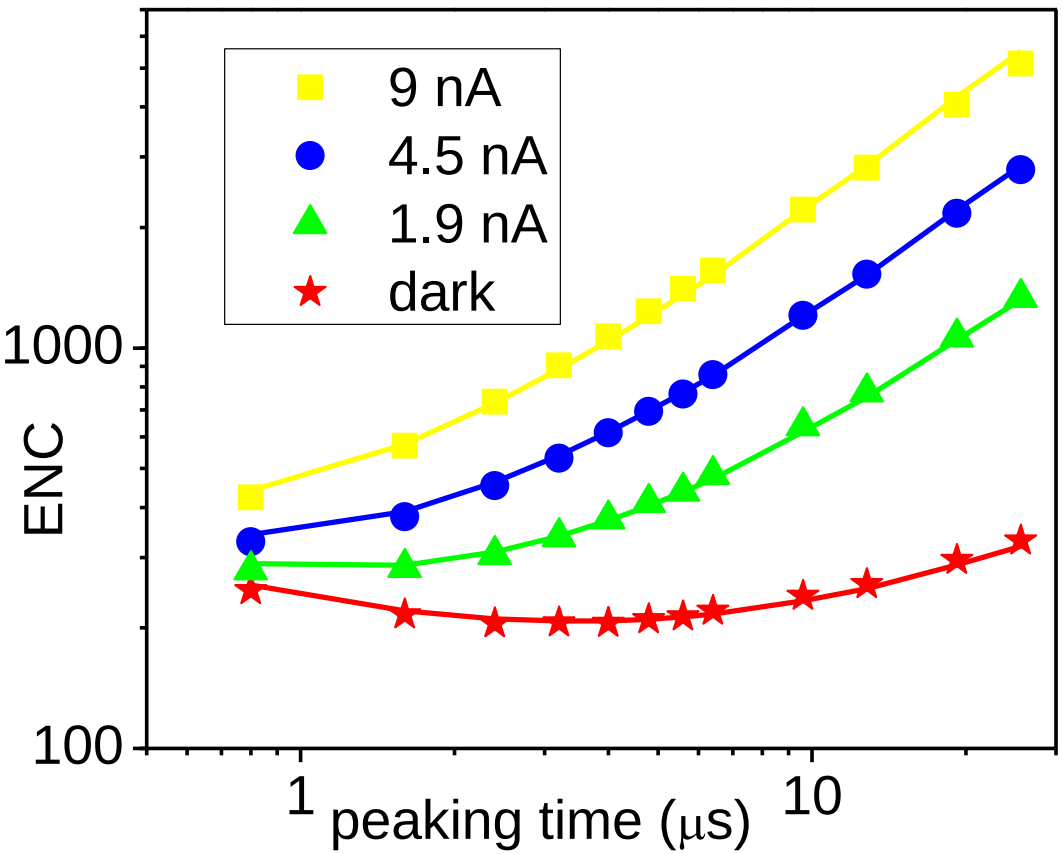

Several Sintef detectors were irradiated with X-rays to increase the oxide charge and prevent the inversion of the silicon surface.

1/f parallel noise: the punch-through current flows quite superficially and holes are trapped by interfacial states

Noise vs V_{gate} in Sintef *p*-side

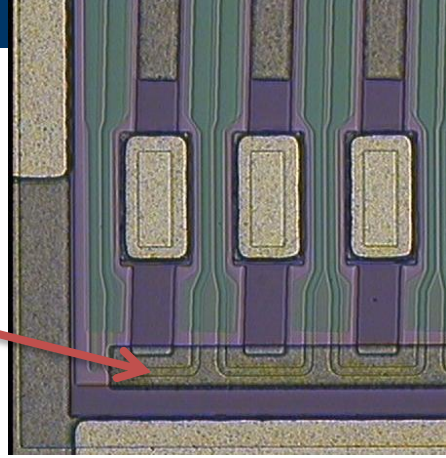

- SINTEF sensors have a metal gate above the P-T region
  → Contacted and biased externally

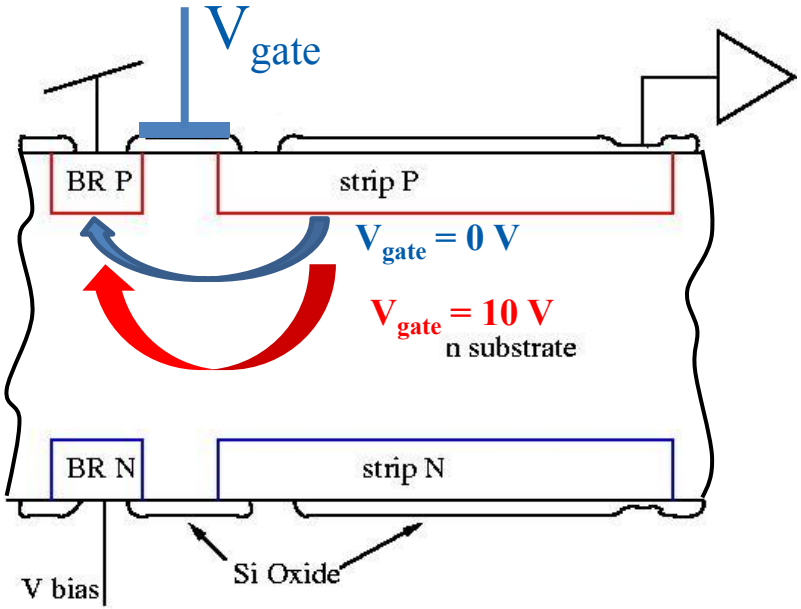

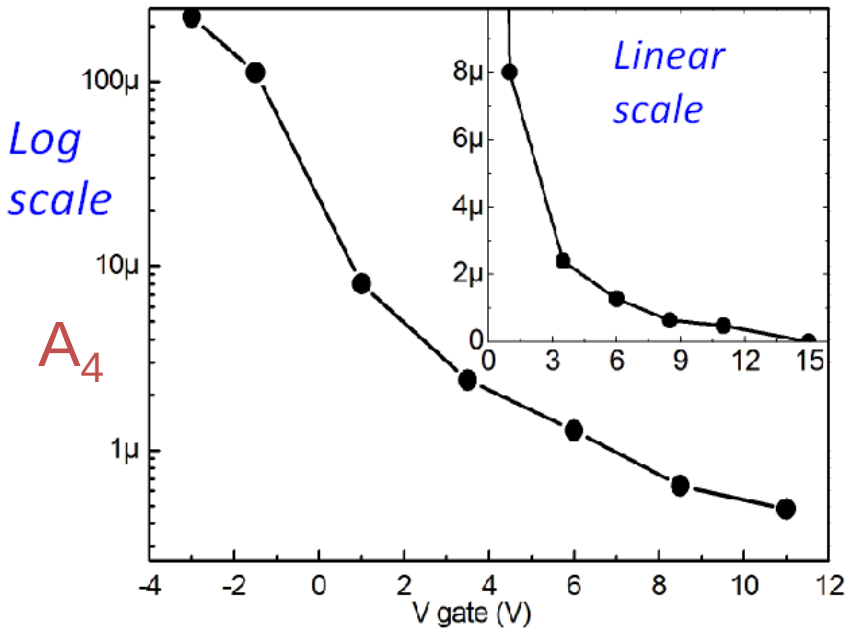

Positive V_{gate} pushes the P-T hole current away from the surface, suppressing the excess noise $ENC^2 = A_4 \; I_{P\text{-}T}^2 \; \tau^2$

Outline

- silicon sensor activity in FBK
- excess noise in silicon microstrip detectors:
  - $ENC^2 \sim sqrt(\tau)$
  - $ENC^2 \sim I^2_{PT}\,\tau^2$
  - thermal noise

Noise induced by p-stop
→ Thermal noise

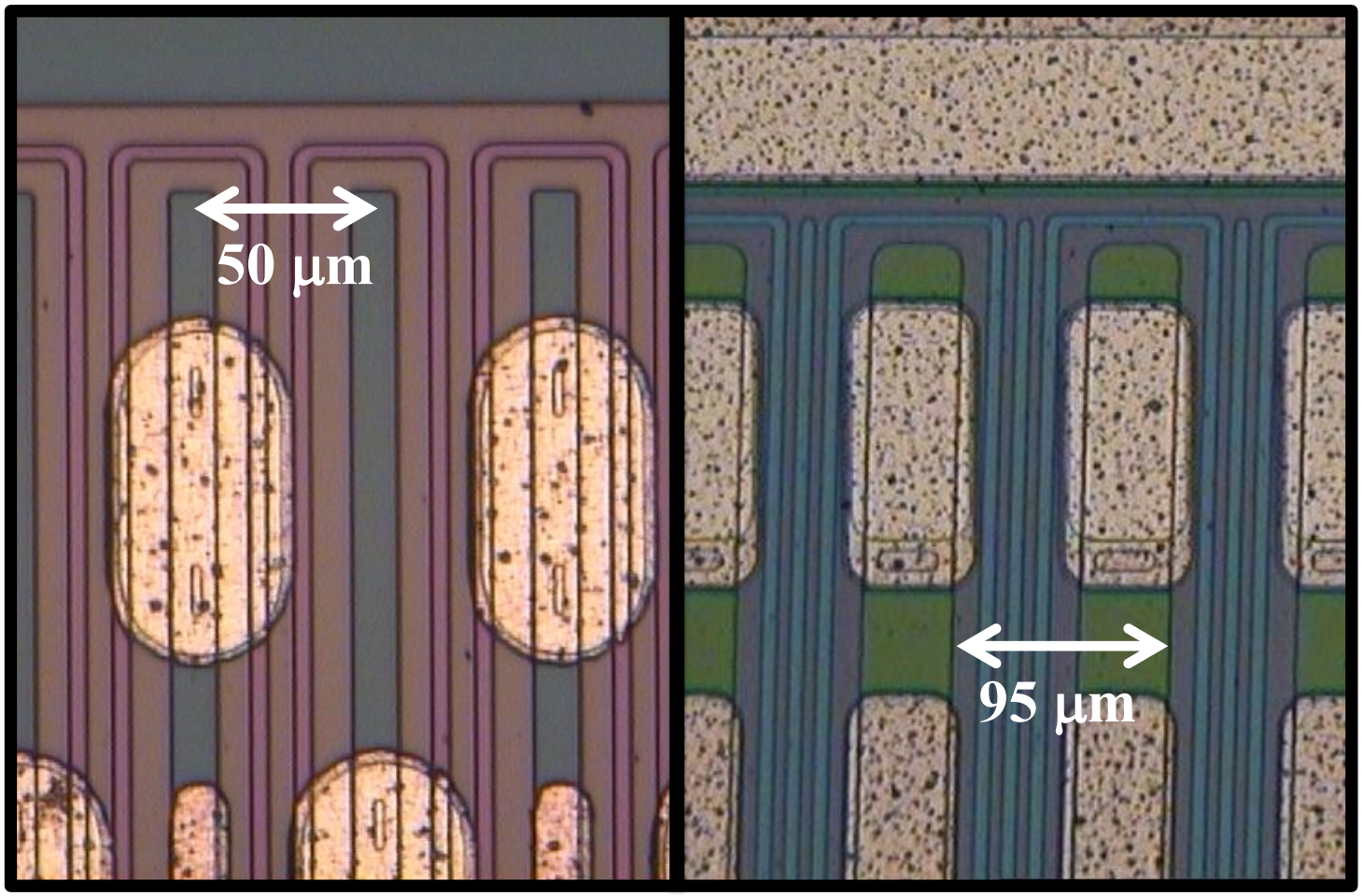

FBK "Telescope" *n*-side

FBK "ALICE" *n*-side

Noise vs τ, vs V_{bias}

FBK "Telescope" *n*-side

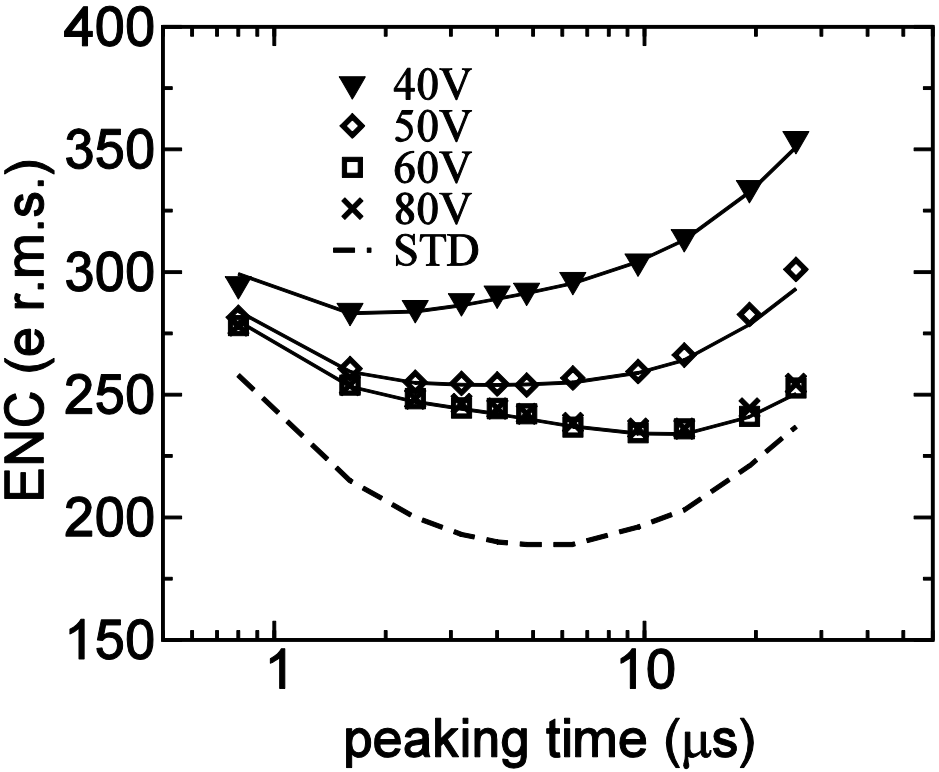

FBK "ALICE" *n*-side

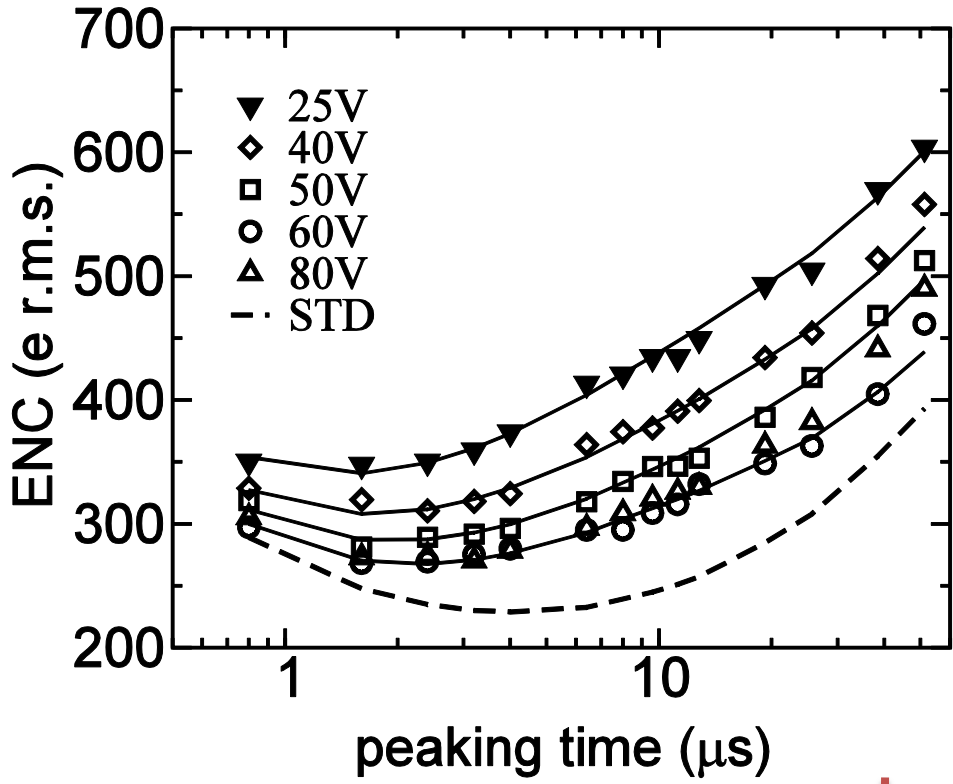

Contribution from $ENC^2 \propto \sqrt{\tau}$
but not enough

"Telescope" *n*-side

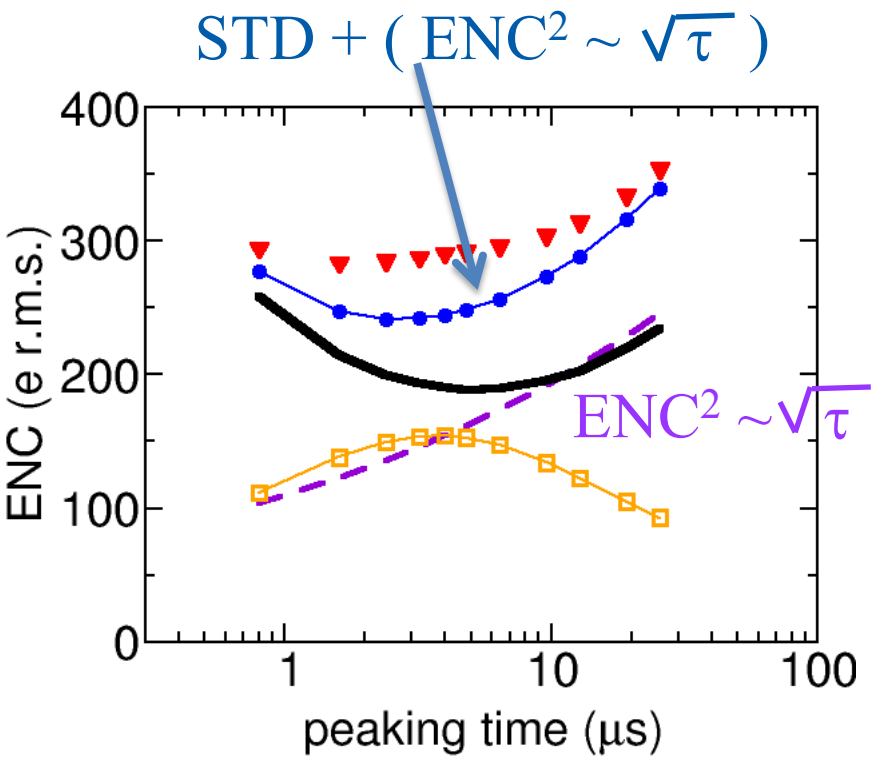

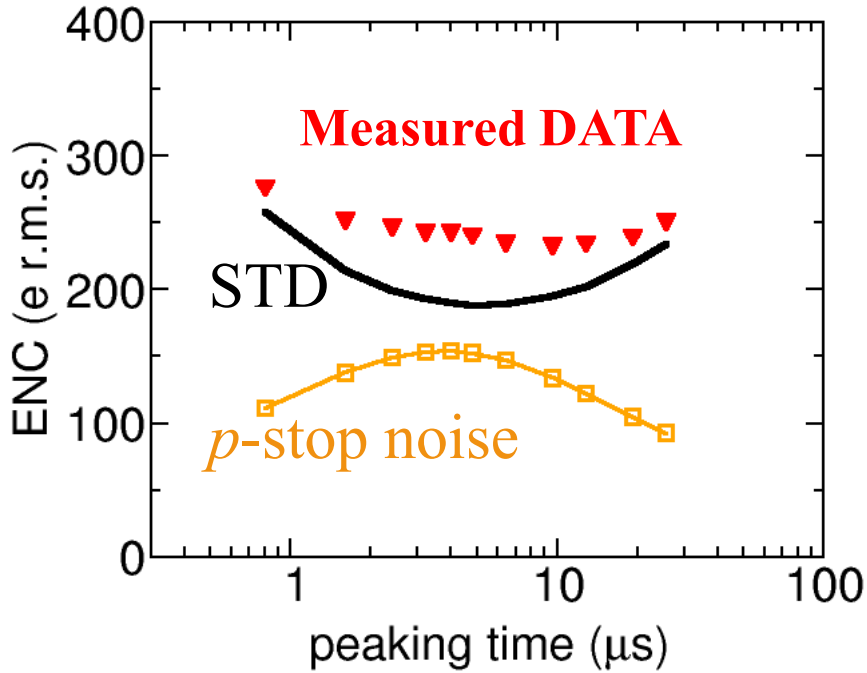

40V: still contribution from resistive layers

60V : no more contribution from resistive layers

The thermal noise of the *p*-stop: $\frac{dv^2}{df} = 4kTR$

is filtered through an RC $\frac{dv^2_{filter}}{df} = \frac{4kTR}{1+(RC*\omega)^2}$

and finally coupled to the strip: $\frac{di^2}{df} = \frac{dv^2_{filter}}{df}\omega^2 C^2_{strip} = \frac{4kTR}{1+(RC*\omega)^2}\omega^2 C^2_{strip}$

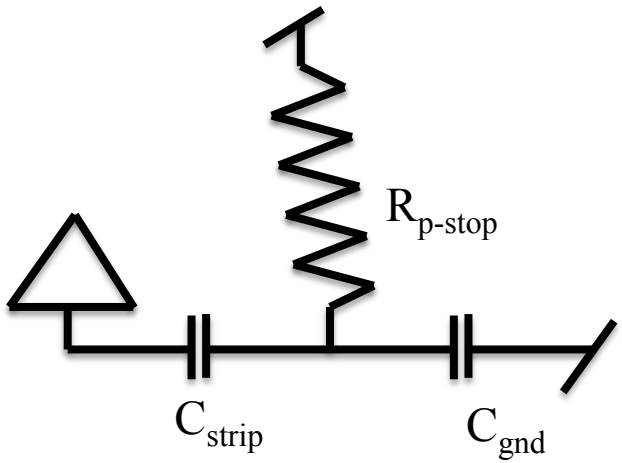

$C_{gnd}+C_{strip}=C$

Filtering the di^2/df through the (triangular) shaper, we get:

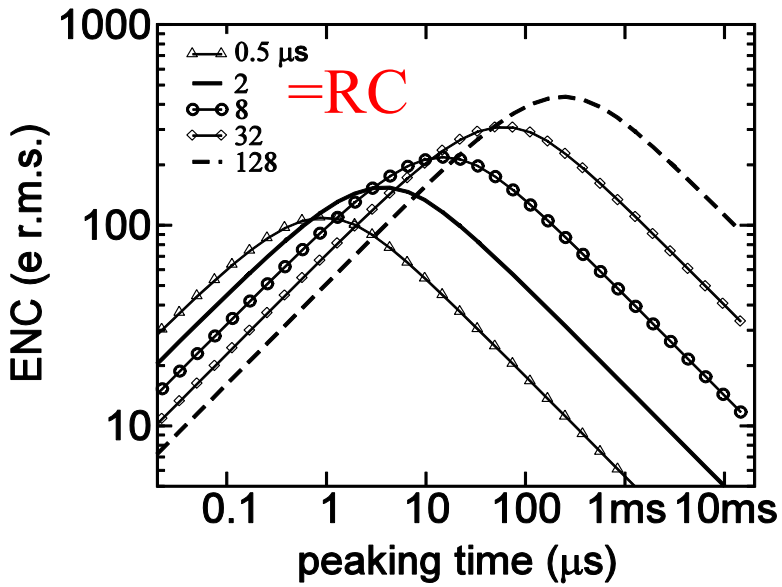

G. Giacomini, L. Bosisio, and I. Rashevskaya, "Measurement of Johnson Noise Induced by *p*-stops in Silicon Microstrip Detectors", *IEEE TNS,* VOL. 60, NO. 5, 2013, pag 4022